AD-A086 049 AIR FORCE MATERIALS LAB WRIGHT-PATTERSON AFB OH F/G 21/5
SOFT BODY IMPACT OF CANTILEVER BEAMS.(U)
MAR 80 J D SHARP
UNCLASSIFIED AFML-TR-79-4169 NL

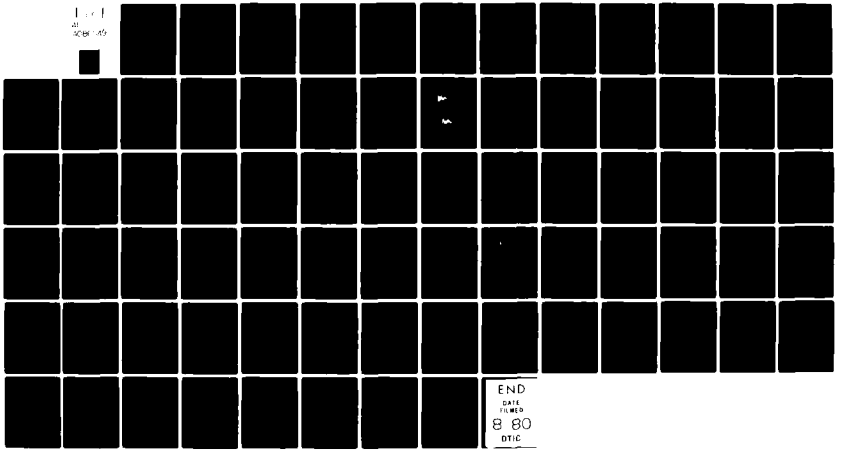

END
DATE FILMED
8 80
DTIC

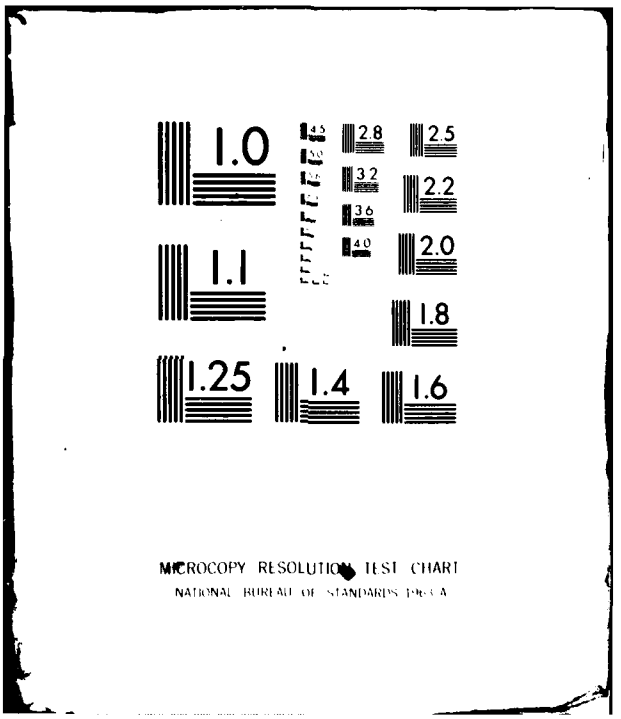
1.0
1.1
1.25
1.4
1.6
1.8
2.0
2.2
2.5
2.8
3.2
3.6
4.0
MICROCOPY RESOLUTION TEST CHART
NATIONAL BUREAU OF STANDARDS 1963-A

AFML-TR-79-4169

SOFT BODY IMPACT OF CANTILEVER BEAMS

Jeffry D. Sharp
Metals Behavior Branch
Metals and Ceramics Division

March 1980

TECHNICAL REPORT AFML-TR-79-4169

Interim Report for Period October 1977 - July 1979

Approved for public release, distribution unlimited.

AIR FORCE MATERIALS LABORATORY
AIR FORCE WRIGHT AERONAUTICAL LABORATORIES
AIR FORCE SYSTEMS COMMAND
WRIGHT-PATTERSON AIR FORCE BASE, OHIO 45433

NOTICE

When Government drawings, specifications, or other data are used for any purpose other than in connection with a definitely related Government procurement operation, the United States Government thereby incurs no responsibility nor any obligation whatsoever; and the fact that the government may have formulated, furnished, or in any way supplied the said drawings, specifications, or other data, is not to be regarded by implication or otherwise as in any manner licensing the holder or any other person or corporation, or conveying any rights or permission to manufacture, use, or sell any patented invention that may in any way be related thereto.

This report has been reviewed by the Information Office (OI) and is releasable to the National Technical Information Service (NTIS). At NTIS, it will be available to the general public, including foreign nations.

This technical report has been reviewed and is approved for publication.

THEODORE NICHOLAS
Project Engineer
Metals Behavior Branch
Metals and Ceramics Division

NATHAN G. TUPPER, Chief
Metals Behavior Branch
Metals and Ceramics Division

"If your address has changed, if you wish to be removed from our mailing list, or if the addressee is no longer employed by your organization please notify AFWAL/MLLN *,W-PAFB, OH 45433 to help us maintain a current mailing list".*

Copies of this report should not be returned unless return is required by security considerations, contractual obligations, or notice on a specific document.

AIR FORCE/56780/18 June 1980 — 400

SECURITY CLASSIFICATION OF THIS PAGE (When Data Entered)

REPORT DOCUMENTATION PAGE

READ INSTRUCTIONS BEFORE COMPLETING FORM

1. REPORT NUMBER: AFML-TR-79-4169	2. GOVT ACCESSION NO.: AD-A086 049
3. RECIPIENT'S CATALOG NUMBER:	
4. TITLE (and Subtitle): SOFT BODY IMPACT OF CANTILEVER BEAMS,	5. TYPE OF REPORT & PERIOD COVERED: Interim Technical Report, Oct 77 — Jul 79,
	6. PERFORMING ORG. REPORT NUMBER:
7. AUTHOR(s): Jeffry D. Sharp	8. CONTRACT OR GRANT NUMBER(s): In-House
9. PERFORMING ORGANIZATION NAME AND ADDRESS: Air Force Materials Laboratory (LLN) / AF Wright Aeronautical Laboratories (AFSC) / Wright-Patterson Air Force Base, Ohio 45433	10. PROGRAM ELEMENT, PROJECT, TASK AREA & WORK UNIT NUMBERS: 2418 03 02
11. CONTROLLING OFFICE NAME AND ADDRESS: Air Force Materials Laboratory (LLN) / AF Wright Aeronautical Laboratories (AFSC) / Wright-Patterson Air Force Base, Ohio 45433	12. REPORT DATE: Mar 80
	13. NUMBER OF PAGES: 76
14. MONITORING AGENCY NAME & ADDRESS (if different from Controlling Office)	15. SECURITY CLASS. (of this report): Unclassified
	15a. DECLASSIFICATION/DOWNGRADING SCHEDULE

16. DISTRIBUTION STATEMENT (of this Report)

Approved for public release; distribution unlimited.

17. DISTRIBUTION STATEMENT (of the abstract entered in Block 20, if different from Report)

18. SUPPLEMENTARY NOTES

19. KEY WORDS (Continue on reverse side if necessary and identify by block number)

Soft Body
Cantilever Beam
Impact
Vibration
Normal Modes
Dynamic Response

20. ABSTRACT (Continue on reverse side if necessary and identify by block number)

Damage incurred by gas turbine engine fan blades due to foreign object ingestion is of great concern to both manufacturers and the agencies that purchase such products. Of particular interest is the response of a structure impacted by a soft body, such as a bird. As a result, efforts have been made in the last several years to understand the dynamic behavior of blade-like structures under impact loading. A great deal of information is available concerning the hard body impact problem. However, the soft body impact problem has not yet been

DD FORM 1 JAN 73 1473 EDITION OF 1 NOV 65 IS OBSOLETE

SECURITY CLASSIFICATION OF THIS PAGE (When Data Entered)

012320

investigated as thoroughly. This study experimentally and analytically investigates the stress/time response of a cantilever beam subjected to impact loading from a soft object. Results from several different analytical models employing the Euler-Bernoulli Beam Theory are compared to experimental data, and the validity of each model is assessed. The effects of structural damping, beam dimensions and the Timoshenko Theory parameters are discussed and conclusions as to their importance are drawn. It was determined that a cantilever beam impacted by a soft body can be accurately modeled as a forced vibration problem using the Euler-Bernoulli Theory and linear modal analysis with damping. In addition, it was shown that large structures can be linearly scaled down for impact testing without affecting the results.

FOREWORD

This work reported herein performed at the Metals Behavior Branch, Metals and Ceramics Division, Air Force Materials Laboratory. The work was performed under in-house Project No. 241803, "Dynamic Behavior of Engine Materials." The work was conducted by Mr. Jeffry D. Sharp, collocated from ASD/ENFSM, Wright-Patterson AFB, Ohio.

The author would like to offer thanks to his thesis advisor, Dr. George Sutherland, Ohio State University, for his suggestions and guidance throughout this work, to Dr. Theodore Nicholas, AFML/LLN, for making available the experimental facilities and providing technical advice, and to Ms. Barbara Lear, ASD/ENF for her secretarial assistance.

The research was conducted during the period October 1977 to July 1979. This report was submitted for publication in September 1979.

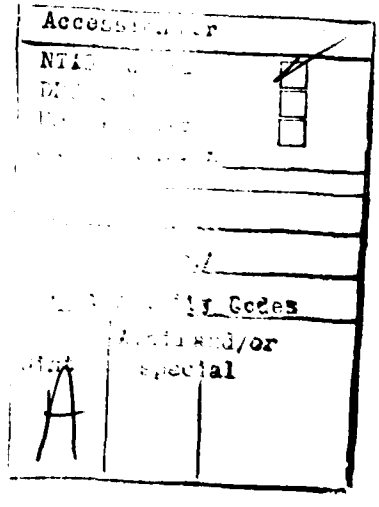

TABLE OF CONTENTS

LIST OF ILLUSTRATIONS

LIST OF TABLES

LIST OF SYMBOLS

D_p	Diameter of Projectile; in.
ρ_p	Density of Projectile; lbm/in.^{3}
V_p	Velocity of Projectile; fps
M_p	Mass of Projectile; lbm
ρ_B	Density of Beam; lbm/in.^{3}
A_B	Cross-Sectional Area of Beam; in.^{2}
M_B	Mass of Beam
ℓ	Length of Beam; in.
E	Modulus of Elasticity of Beam; lbf/in.^{2}
I	Moment of Inertia of Beam Cross Section; in.^{4}
L	Spanwise Location of Impact; in.
T_0	Duration of Impact; sec.
$\phi(x)$	Mode Shape Function for Cantilever Beam; in.
ξ	Modal Damping Factor
ε	Strain; in./in.

SUMMARY

With thrust-to-weight ratios in aircraft gas turbine engines increasing, all components are required to operate at higher steady-stress levels. This situation, coupled with cyclic life limits based on crack propagation, demands a better understanding of the operating environment and various loading conditions to which a component may be subjected throughout its useful life. Vibratory stresses induced in rotating airfoils by foreign object impacts are a real part of jet engine operating environments and require careful consideration when designing high performance blades. However, before one can analyze a component for such conditions, the loading mechanism must be understood. This has been investigated for members of similar stiffnesses impacting each other (References 1 through 4), but little work has been done to define and analyze the effect of a soft body impacting a member with the approximate geometry and stiffness of a fan blade. The first step toward accomplishing this understanding is to fabricate several cantilever beam test specimens, impact them with soft projectiles, and record the strain response at various locations as a function of time. From this data base, a simple beam theory model can be evaluated for several different cases, each treating the impact as a slightly different phenomenon, but based on the common assumption that all the projectile momentum is transferred to the beam. The results indicate that a soft-body impact on a cantilever beam can be modeled as forced vibration for the duration of the impact, then free vibration for all time thereafter. The forcing function created by the projectile is best modeled as a step-function distributed over an area. Damping in the system has a significant effect on strain in the beam, but is difficult to accurately predict, and thus should not be considered in maximum strain calculations. However, an accurate strain/time history can be predicted if modal damping values for the first four resonant modes are known. Impact testing of very large structures can be performed on scaled down models with no change in results.

SECTION I

INTRODUCTION

The problem of predicting the response of a blade-like structure to an impact by a soft body is very complex and involves many structural interactions. To begin analyzing all the load transfer mechanisms present in such a problem is a monumental task. One must initially take a more basic approach. The objective of this study is to determine how a simple cantilever beam responds to an impact on its centerline by a soft object. If the overall bending strain at various spanwise locations in a beam can be recorded throughout an impact, the gross loading mechanism can be studied and an analytical model can be developed to predict the response.

To accomplish this objective, four geometrically similar beams were fabricated and instrumented with strain gages at various spanwise locations, mounted in a cantilever configuration, and impacted with geometrically similar soft projectiles. Data from the strain gages was digitally recorded during impact, stored, then analyzed to determine maximum strain at each gage location and the modal content of each response. Any damping effects present were noted. This provided the dynamic response data necessary to evaluate several proposed analytical models.

Next, analytical models based on the Euler-Bernoulli Beam Theory and employing linear modal analysis were formulated. Two basic approaches were used to simulate the impact loading. The first was to assume a purely impulsive loading in which the projectile imparted an instantaneous initial velocity to the beam. The second treated the impact as a forced vibration problem, which modeled the impact as a.) a step function and b.) a half sine wave in time. Each model was defined and formulated on a computer and the resulting time responses were compared with the test data to determine its accuracy. The following text describes in detail the experimental work performed, the data analysis techniques used, the different model derivations and formulations, and finally, the results obtained from each model and a comparison with experimental results.

SECTION II

EXPERIMENTAL PROCEDURE AND RESULTS

Four cantilever beam specimens were fabricated from 7075 T-6 aluminum, approximately 91 R or 190 B hardness, the smallest beam being 5.6 inches long, 1.2 inches wide, and 0.15 inches thick. The remaining beams were scaled from these dimensions by factors of 1.5, 2.0, and 2.5. To ensure cantilever boundary conditions and minimize damping effects from mounting fixtures, the root section of each specimen was left significantly thicker than the rest of the beam, as shown in Figure 1.

For simplicity, the impact site of each beam was chosen to be at 75% span. This provided a reasonable portion on either side of the desired impact location to ensure contact by the whole projectile. Strain gages were mounted on each beam at the root and 75% span on the side opposite that to be impacted. On three of the four beams, gages were also placed at 25% and 50% span to record additional data (Figure 2). These four locations were chosen to help identify the location of maximum strain and to provide a sufficient amount of strain/time history information to facilitate verification of analytical models.

The projectiles used to impact each beam were spherical bodies of micro-balloon gelatin, a porous gelatin used to simulate bird impacts (Reference 7). Projectile sizes and velocities were selected to meet several criteria. The base line projectile diameter was chosen to be 0.5 inches so it would be small compared to the smallest beam length and width. The geometric ratios used to size the beams were also used to determine the remaining projectile diameters. This calculation yielded projectile diameters of 0.5, 0.75, 1.0, and 1.25 inches. However, a 0.75 inch diameter mold was not available, so the projectile sizes actually used for the impact experiments were 0.5, 0.70, 1.0, and 1.25 inches in diameter. A calculation was made for approximating projectile velocities based on a one degree-of-freedom lumped mass beam model (Reference 6). To assure elastic response, velocity calculations were based on 0.25% strain at the beam root, which predicted a projectile velocity of about 570 fps. These calculations are detailed

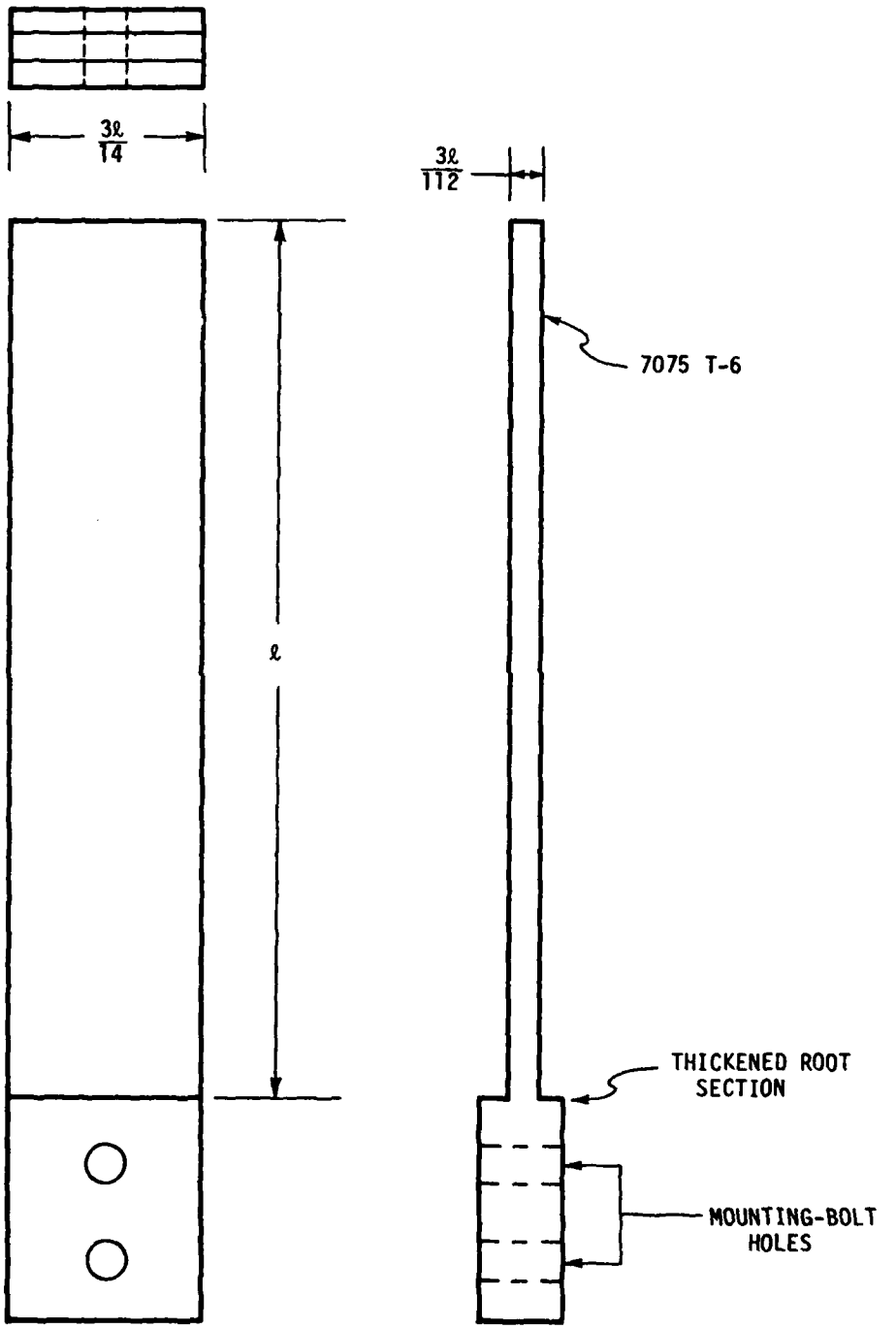

Figure 1. Schematic of Cantilever Beam Specimens

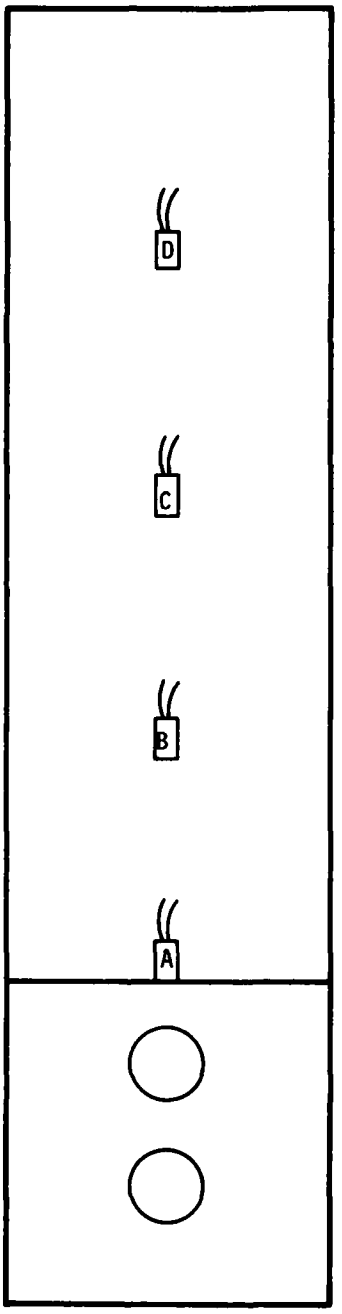

A - ROOT LOCATION: ALL BEAMS

B - 25% SPAN; 5.6, 11.2, & 14.0

C - 50% SPAN; 5.6, 11.2, & 14.0

D - 75% SPAN: ALL BEAMS

Figure 2. Strain Gage Placement on Beams

in Appendix A. To account for the gross model used, the velocity prediction was decreased to 400 fps. An attempt was made to maintain this projectile velocity for each beam specimen so the concept of scaling impact specimens could be investigated.

Two different devices were used to record transient strain data. A Hewlett-Packard 5451B Fast Fourier Analyzer (FFT) capable of digitizing and storing four channels of data at 20 KHZ was employed to provide a record of transient response data which could be analyzed at a later time. A Zonics AE 102-2 transient recorder capable of digitizing eight channels of data from 2 KHZ to 200 KHZ was utilized to investigate short time and long time responses. Strain data recorded by the FFT unit was stored on a magnetic disk, while the transient recorder data was stored temporarily in the recorder and then input to an oscilloscope and photographed.

For testing, each beam was mounted in a steel fixture as shown in Figure 3. The entire assembly was then placed inside a steel enclosure on the impact range, positioned with a laser aiming device and then secured to the enclosure.

Projectiles were first weighed and the weight recorded, and then launched from a smooth-bore tube, propelled by compressed air, compressed helium, or burning gunpowder. Each projectile was carried down the tube in a sabot, a plastic bore fitting carrier, which protected it from the launch tube walls. Several inches in front of the target a constriction in the barrel stopped the sabot, allowing the projectile to continue. Before striking the beam, the projectile tripped a pair of laser light sources connected to a time interval counter to measure its velocity.

Several shots were made at each beam to "zero in" on the amount of pressure/powder necessary to attain the desired velocity. Impacts on the first beam indicated that a velocity between 300 and 350 fps was adequate to produce the desired strain at the specimen root. Thus, those values became bounds on the desired velocity for all remaining tests.

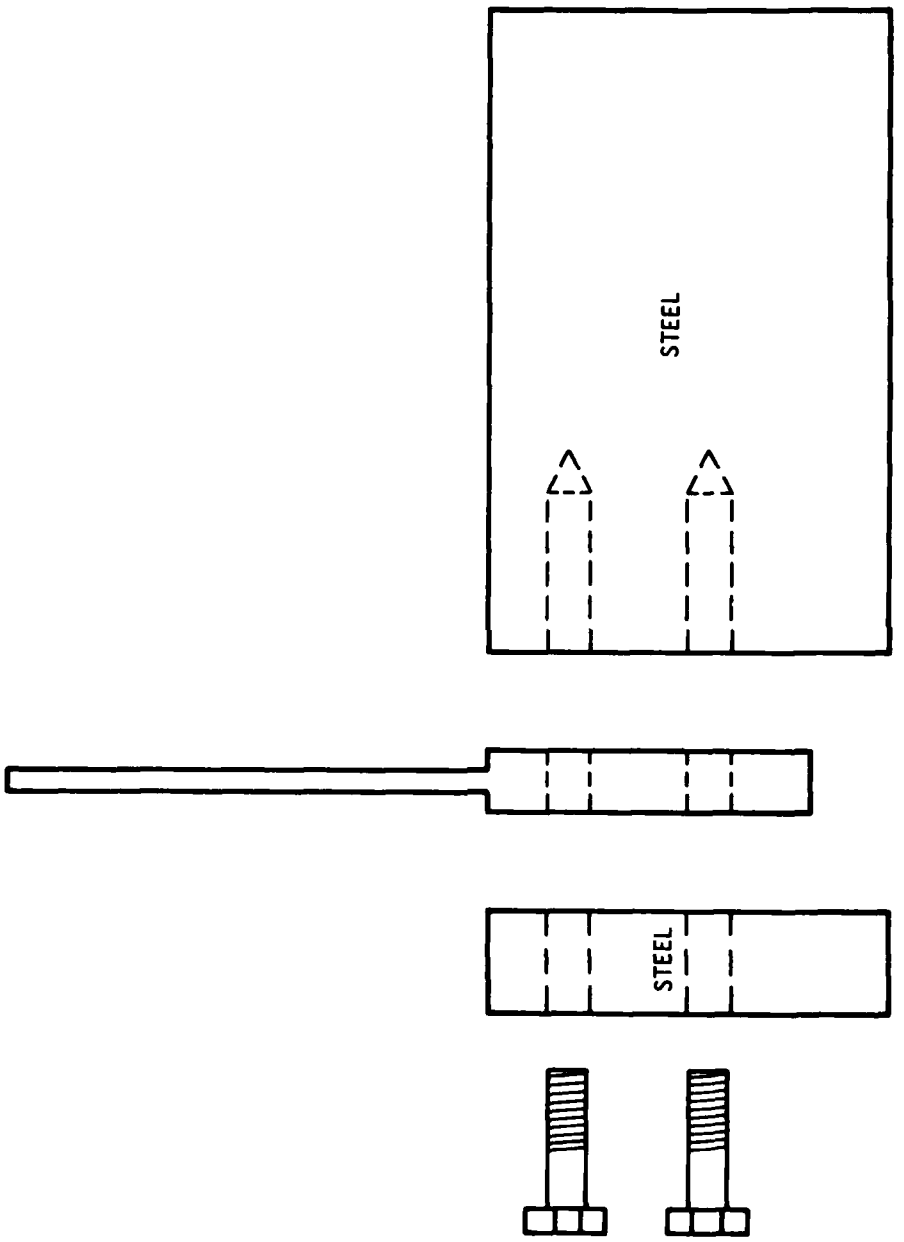

Figure 3. Beam Specimen Mounting Configuration

Figures 4A through 4D are strain/time responses from each beam root location. Variations in peak strain values due to differing projectile velocities and densities can be seen. The data indicates, however, that linear scaling of all beam and projectile dimensions will produce equal strains. Appendix B is a dimensional analysis that supports this observation. Responses from the impact site (75% span) on each beam are shown in Figures 5A through 5C. The same observations made of the root strain data can also be made of these traces. In addition, very little damping effect can be observed in either set of data, except at high frequency. Figures 6A through 6D are the strain responses from each gage location on the 14.0 inch beam. These traces indicate that the maximum strain experienced during impact occurs at the beam root. Figures 7A through 7D show the response of the 14.0 inch beam over 0.5 milliseconds as being slow and containing no high frequency components. Figures 8A through 8D are the responses of the same locations over 500 milliseconds, demonstrating damping in the system affecting only long-term response. All the strain traces indicate the presence of several frequency components. However, it should be noted that the sampling rate used to record this data was too slow to pick up frequencies above the first or second mode. Figures 9A through 9D are Digital Fourier Transforms of root strain responses from each beam, showing the presence of the first four beam bending modes. Similar plots for the 75% span location, Figures 10A through 10C show the same result with a small contribution from the fifth mode. Table 1 summarizes the maximum strain values from all experimental records.

An overview of the test results leads to several conclusions. The maximum stress over the entire impact event occurs at the beam root. For the same projectile velocity and density, linearly scaled beams and projectiles will produce the same impact strain values. The strain response at any location in the beam has significant contribution from only the first five resonant bending modes. Damping in the system has little effect on the peak strain value but does become apparent in long time response. These results provided the basis for evaluating several analytical models.

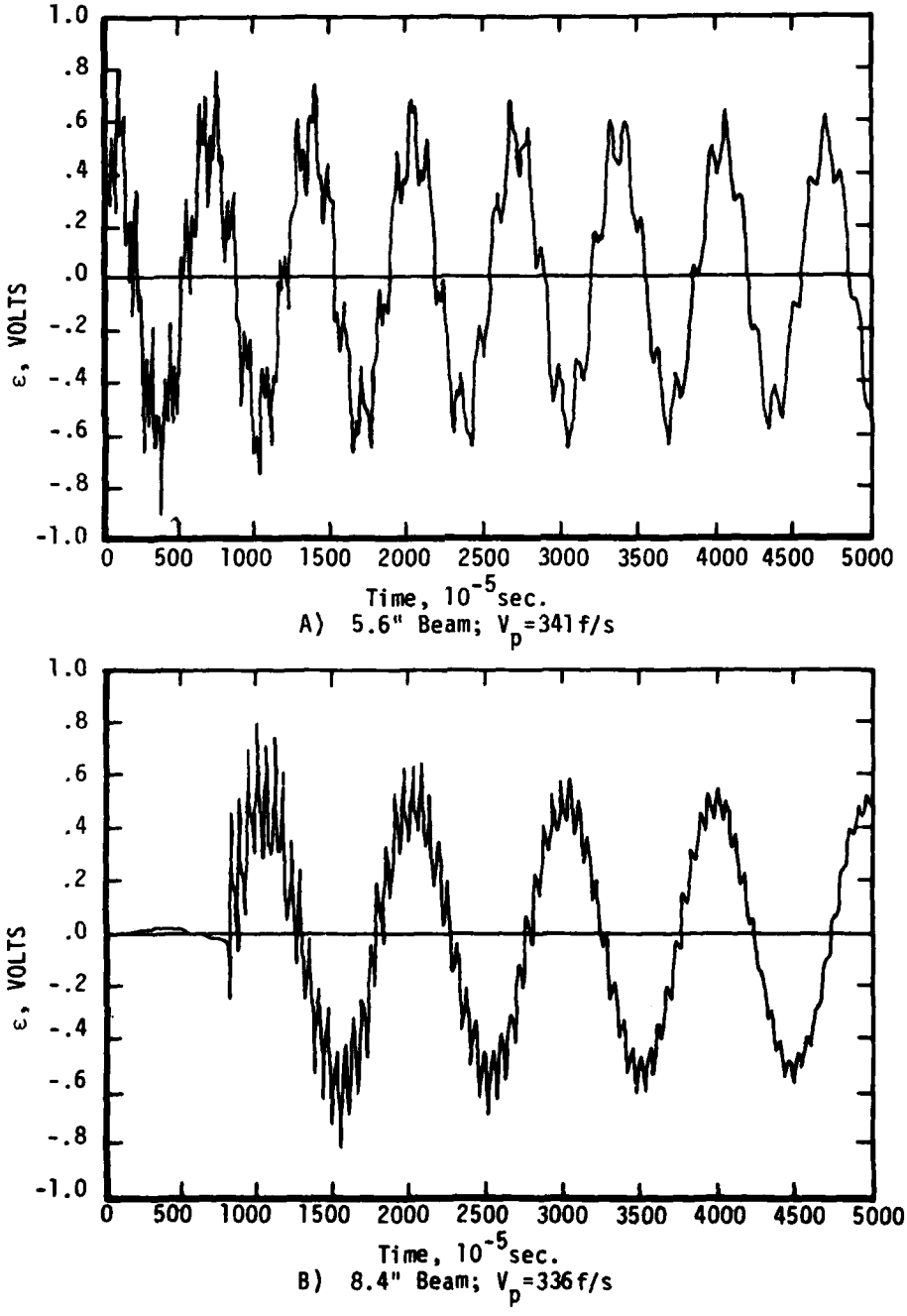

Figure 4. Experimental Strain at Root Location

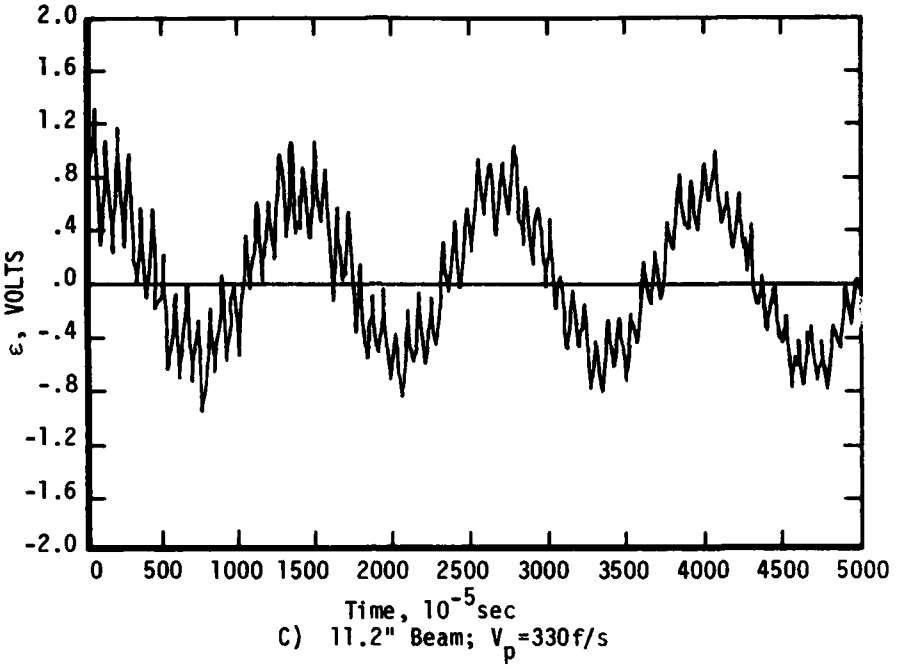

C) 11.2" Beam; V_p=330f/s

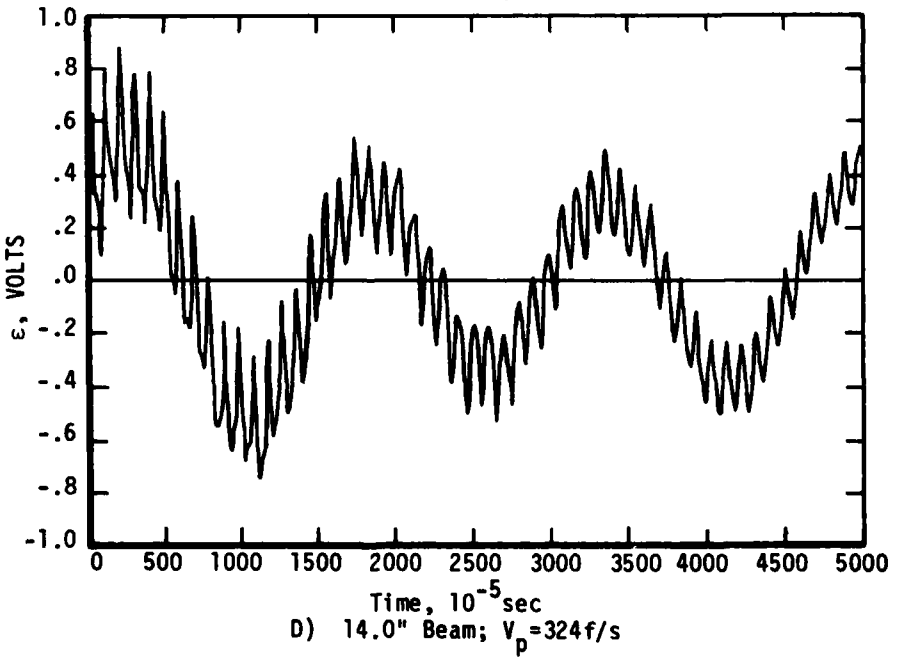

D) 14.0" Beam; V_p=324f/s

Figure 4. (Contd)

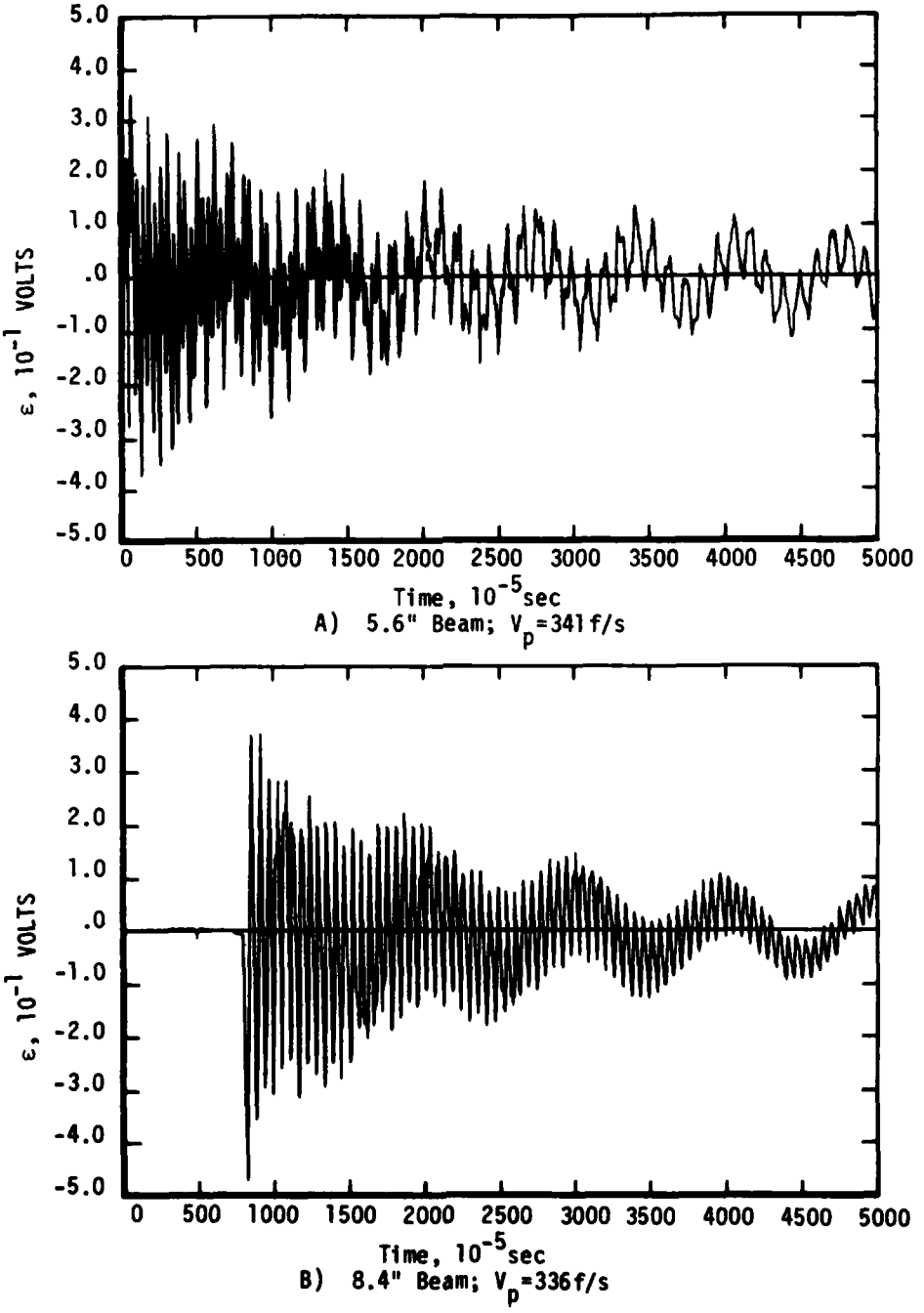

Figure 5. Experimental Strain at Impact Location

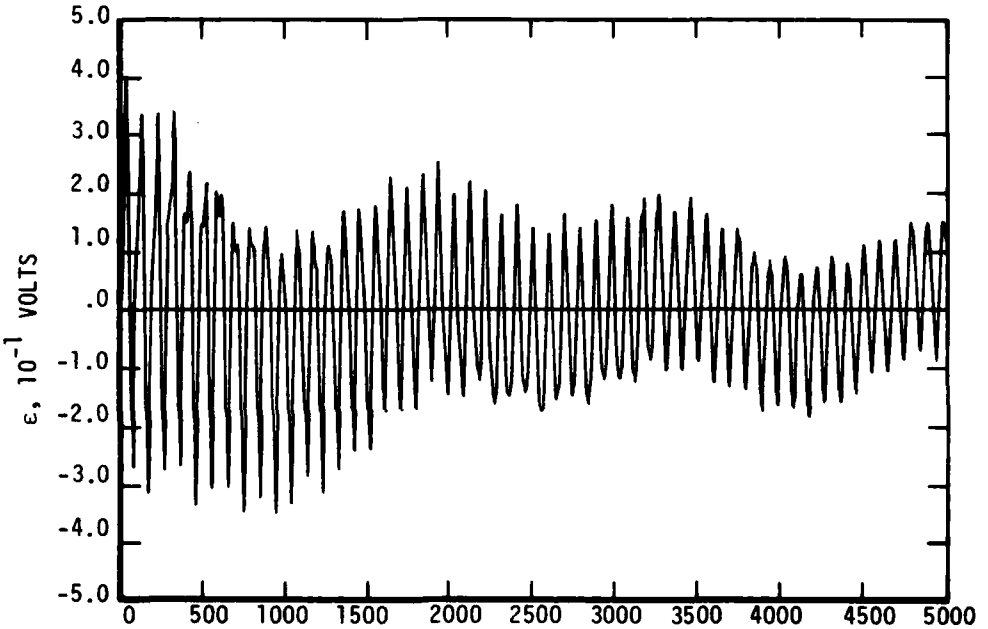

C) 14.0" Beam; V_p=324f/s

Figure 5. (Contd)

*No Data Available At This Location From 11.2" Beam.

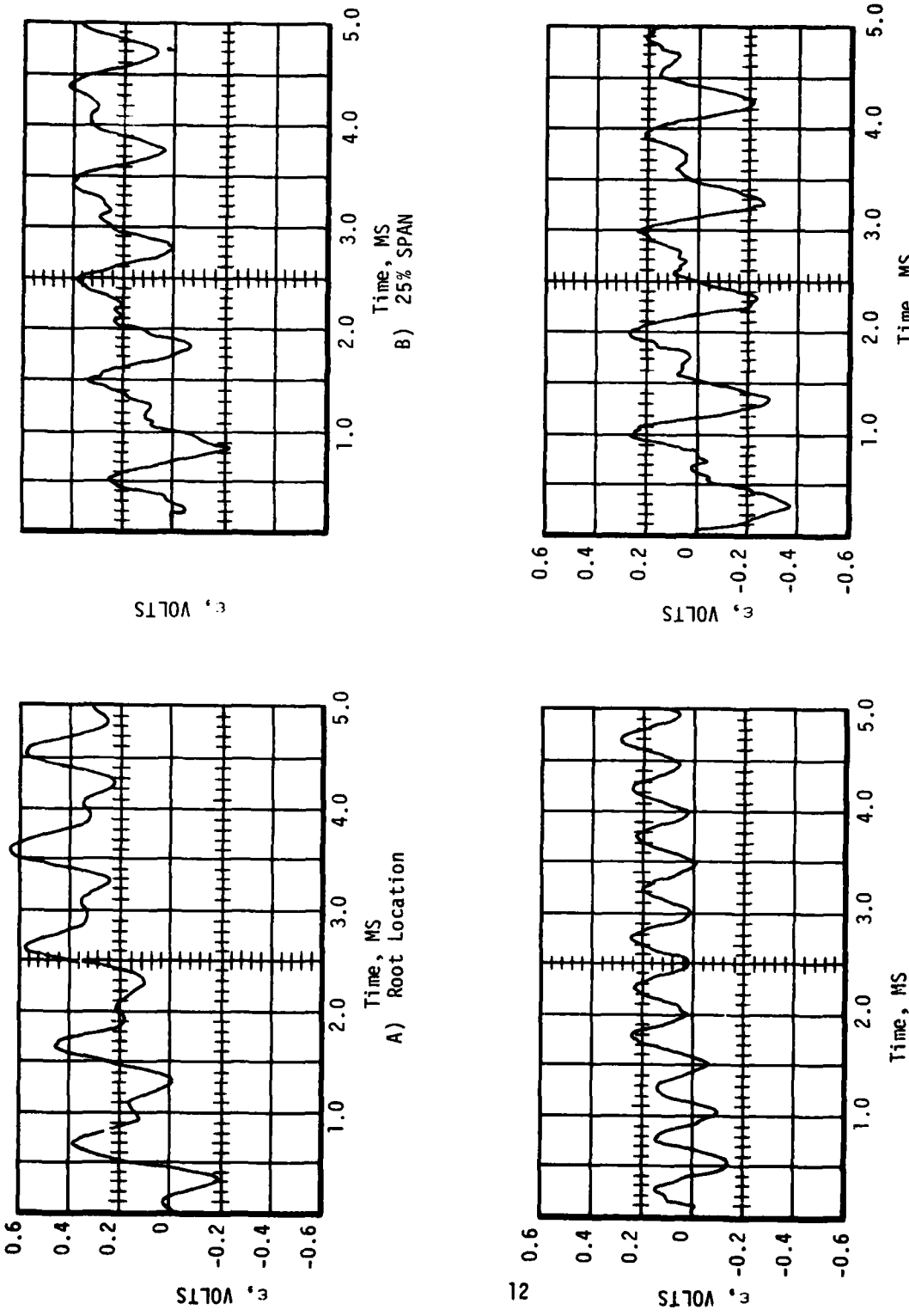

*ρ_p = .0298; V_p = 365 f/s

Figure 6. Experimental Strain in 14.0 Inch Beam (5.0 ms.)

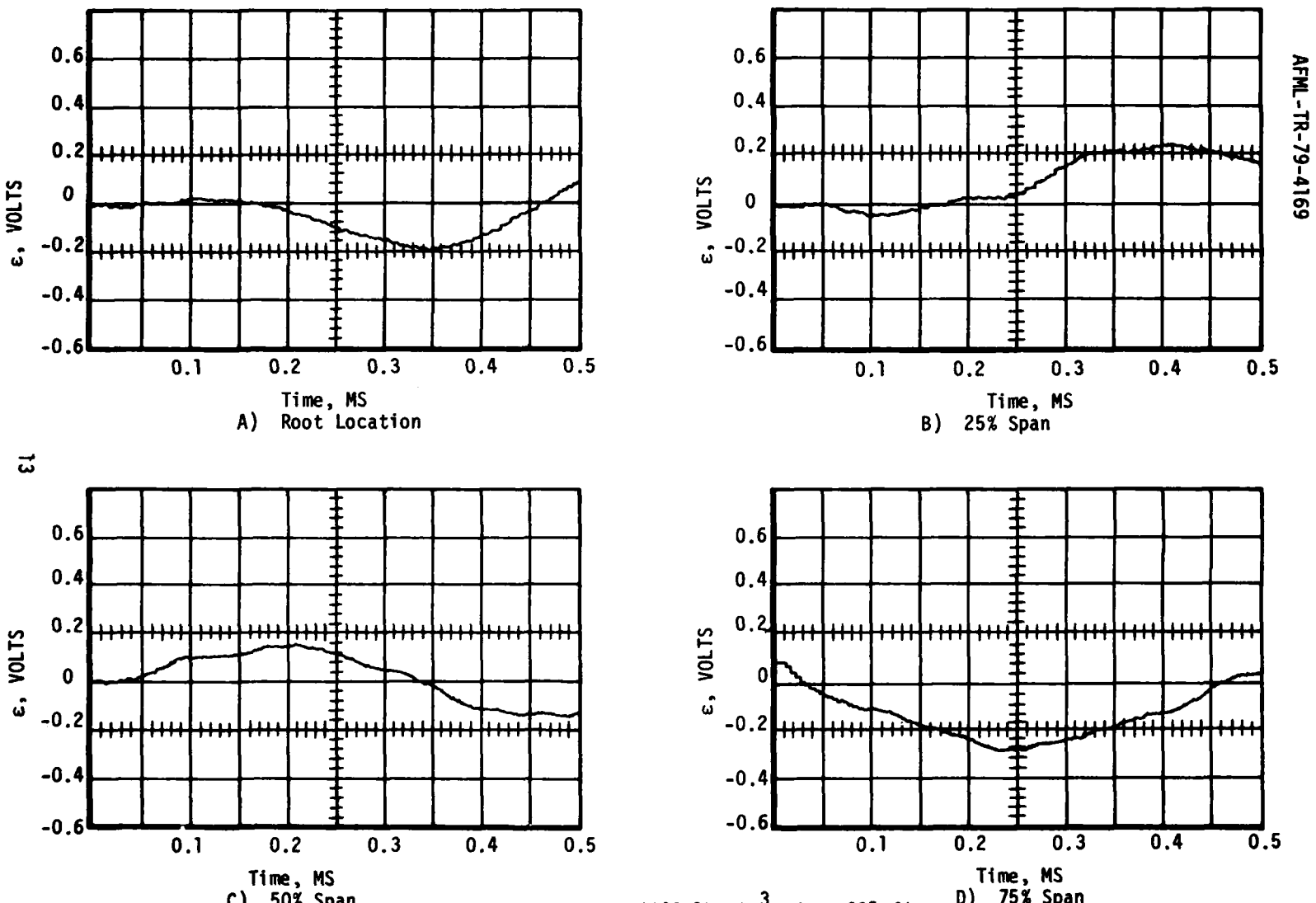

*ρ_p = .0298 lbm/in^3; V_p = 365 f/s

Figure 7. Experimental Strain in 14.0 Inch Beam (0.5 ms.)

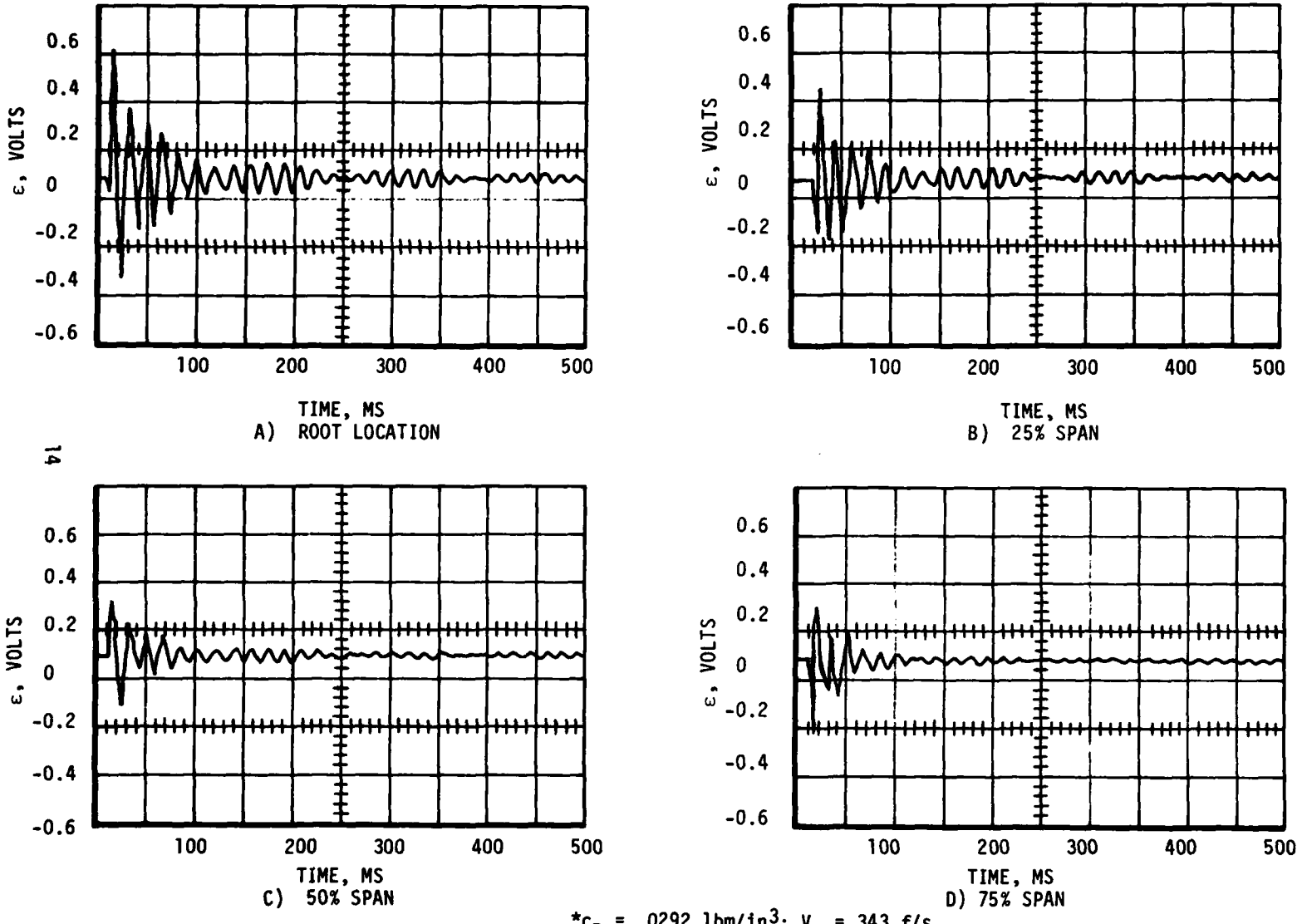

*c_p = .0292 lbm/in^3; V_p = 343 f/s

Figure 8. Experimental Strain in 14.0 Inch Beam (500 ms.)

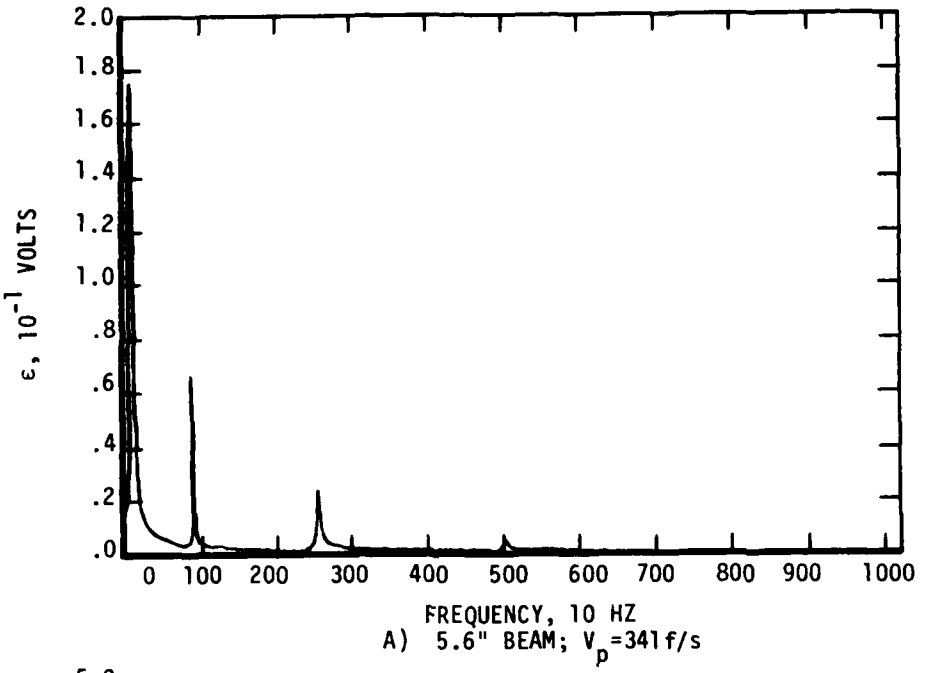

A) 5.6" BEAM; V_p=341f/s

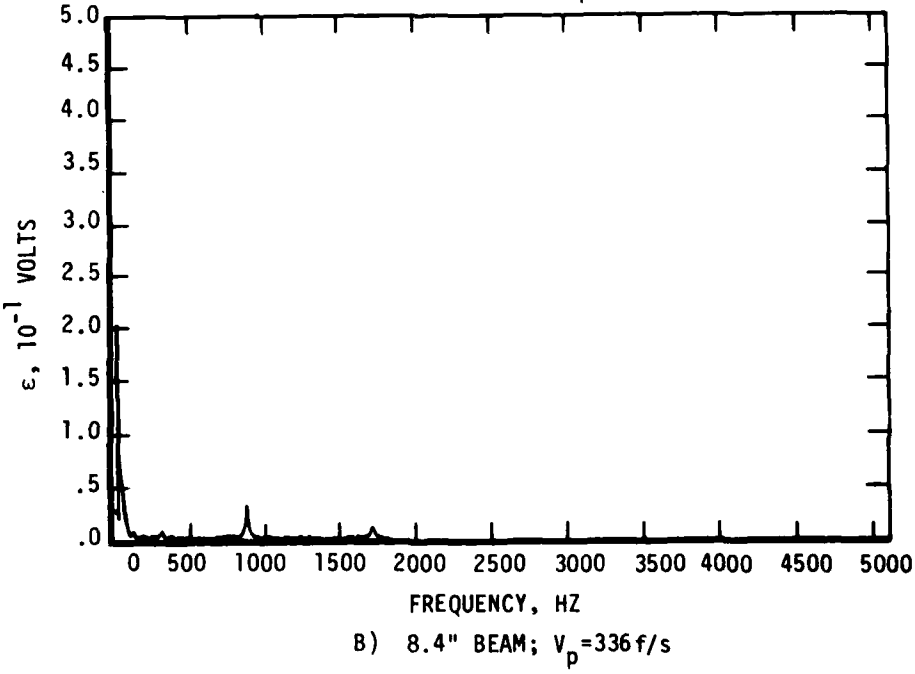

B) 8.4" BEAM; V_p=336f/s

Figure 9. Fourier Transforms of Root Strain Data

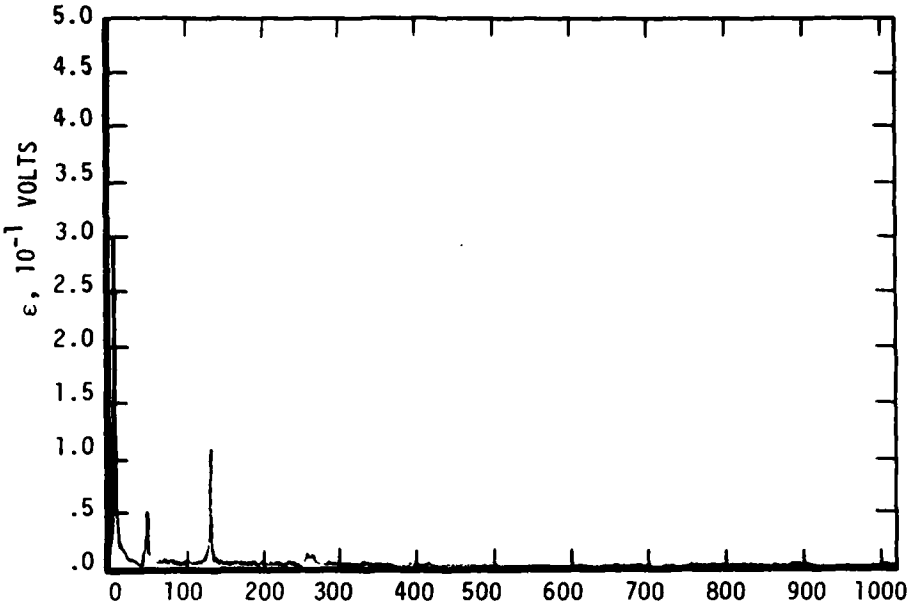

C) 5.6" BEAM: V_p=341f/s

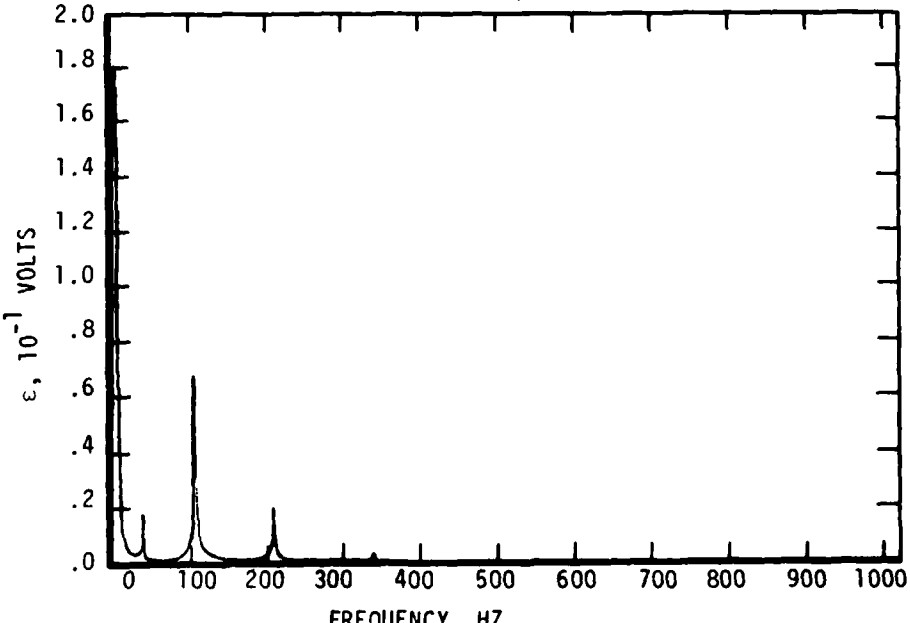

D) 8.4" BEAM: V_p=336f/s

Figure 9. (Cont'd)

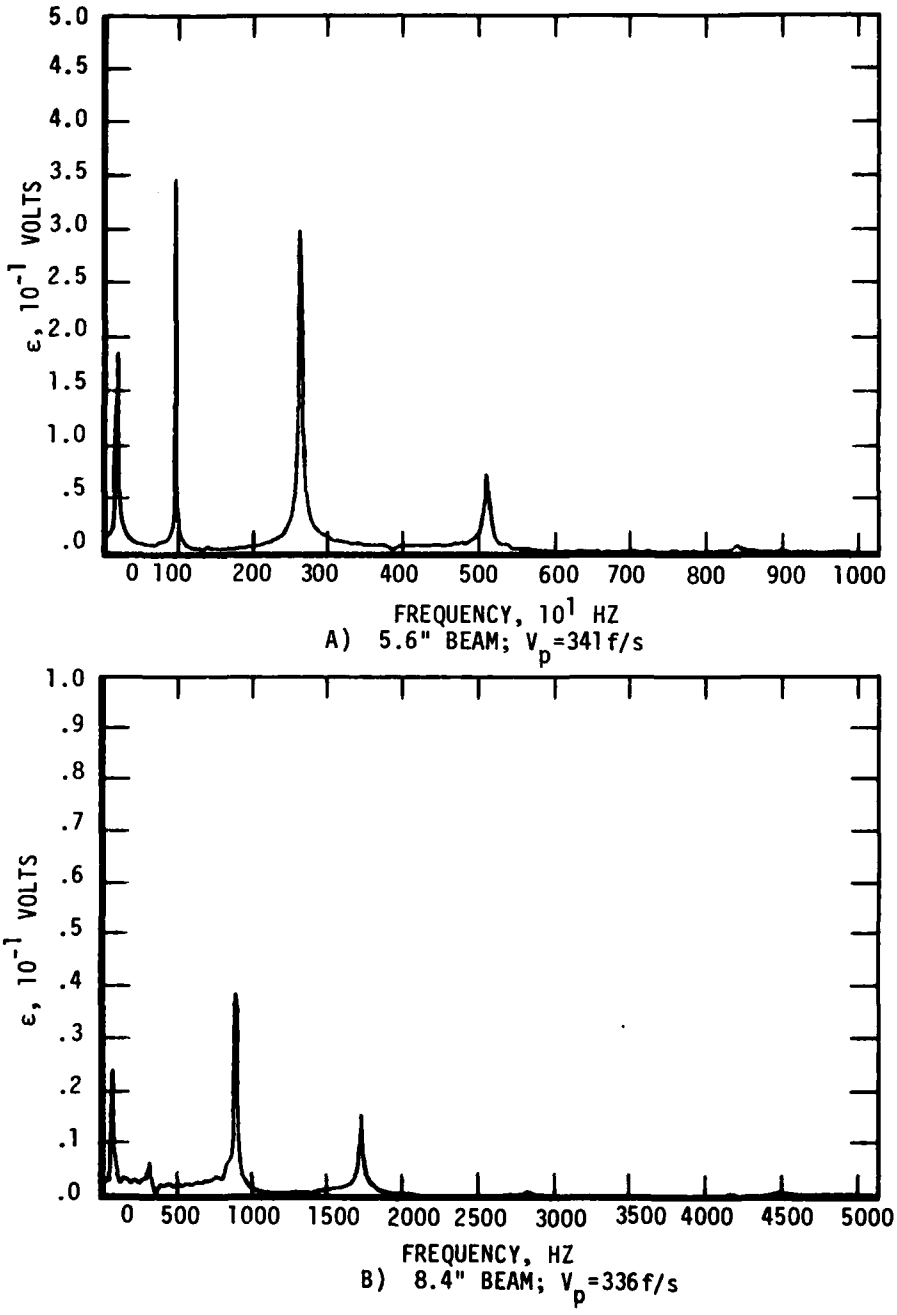

Figure 10. Fourier Transforms of Impact Site Strain Data

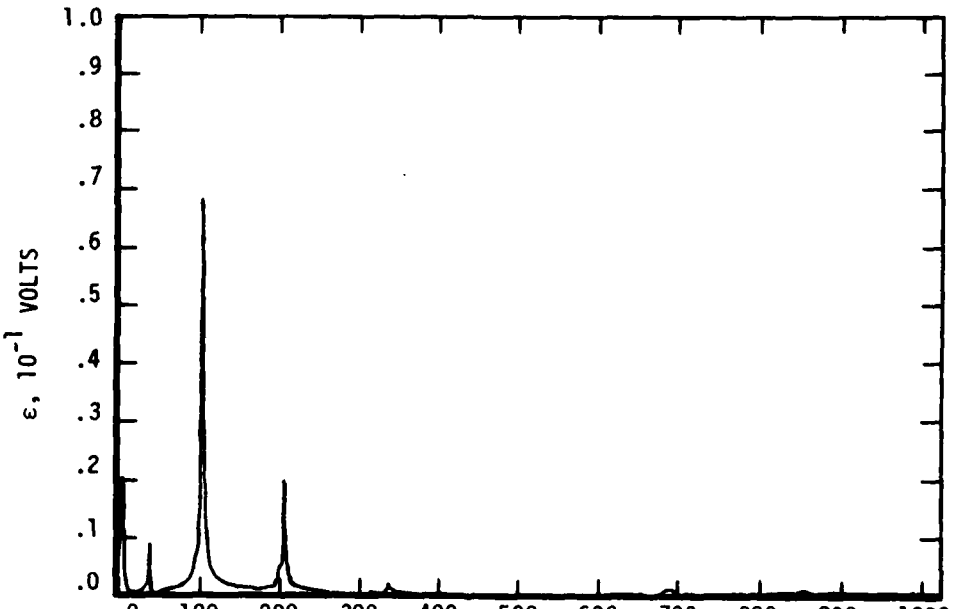

C) 14.0" BEAM; V_p=324f/s

*No Data Available At This Location From 11.2" Beam.

Figure 10. (Cont'd)

TABLE 1

EXPERIMENTAL RESULTS*

Beam Length,in.	D_p, in	V_p, f/s	ε_{root}, %	ε_{25}, %	ε_{50}, %	ε_{75}, %	$t_{max\ \varepsilon}$,s
5.6	0.5	370	0.278	-	-	0.155	1.5
5.6	0.5	341	0.269	-	-	0.113	0.3**
8.4	0.7	344	0.225	-	-	0.134	2.1
8.4	0.7	336	0.231	-	-	0.103	2.1
11.2	1.0	366	0.282	-	-	0.139	2.9
14.0	1.25	365	0.247	0.162	0.116	0.147	3.55
14.0***	1.25	343	0.209	0.154	0.077	0.116	5.0
14.0	1.25	324	0.250	-	0.091	0.114	2.3
14.0	1.25	317	0.254	0.175	0.086	0.105	3.0

* Strains are absolute value.

** Recorder triggered late.

*** Large data point separation; poor strain resolution.

SECTION III

THEORETICAL SOLUTION

Two basic approaches were taken to modeling the soft-body impact problem. The first entailed treating the projectile as imparting an initial velocity to the beam at the point of impact. This approach was suggested in Reference 9 and applied to a hard-body impact problem in Reference 8. The second approach was to treat the beam response to impact as a forced vibration, as in Reference 4. The forcing function was modeled as both a square wave and a half-sine wave. In both formulations, the common assumption made was that all the projectile momentum is transferred to the beam, i.e., linear momentum is conserved and the projectile assumes a velocity of zero after impact. This assumption, which is supported in Reference 7 and by experimental observation, implies that the coefficient of restitution is close to zero, but unknown. Both formulations are based on linear modal theory and employ the Euler-Bernoulli beam relationships. Timoshenko beam effects (i.e., shear and rotary inertia) were investigated and found to be negligible (Appendix C).

The solution for free vibration of a beam developed in Reference 5 was used to determine the resonant frequencies and mode shapes of a cantilever. The general beam mode shape (as a function of space coordinate only) is given by:

$$y(x) = A \sinh(\beta x) + B \cosh(\beta x) + C \sin(\beta x) + D \cos(\beta x) \qquad (1)$$

where β is dependent upon the applied boundary conditions. For a cantilever:

$$\text{at } x = 0: \quad y = 0, \quad dy/dx = 0$$

$$\text{at } x = \ell: \quad M = 0 \text{ or } d^2y/dx^2 = 0, \quad V = 0 \text{ or } d^3y/dx^3 = 0$$

Substitution of these boundary conditions into Equation 1 yields:

$$\cosh(\beta\ell)\cos(\beta\ell) + 1 = 0 \tag{2}$$

which is the solution for βb for the various resonant modes. The mode shape expression can also be rewritten, as a result of applying the boundary conditions, as:

$$y(x) = A\ \{\cosh(\beta x) - \cos(\beta x) - K\ [\sinh(\beta x) - \sin(\beta x)]\} \tag{3}$$

where $k = \sinh(\beta\ell) - \sin(\beta\ell)/\cosh(\beta\ell) + \cos(\beta\ell)$. For simplicity, Equation 3 will be written as:

$$y(x) = A\ \phi(x)$$

defining

$$\phi(x) = \cosh(\beta x) - \cos(\beta x) - K\ [\sinh(\beta x) - \sin(\beta x)] \tag{3a}$$

Employing linear modal theory, the total response of the beam, including time variation, can be formulated as:

$$y(x, t) = \sum_{N=1}^{\infty} A_N \phi_N(x) T_N(t) \tag{4}$$

with $\phi_N(x)$ corresponding to a solution of Equation 3a for a particular value of β, determined from Equation 2. $T_N(t)$ is a time varying function of the resonant frequency for each mode, ω_N, calculated from

$$\omega_N = \beta^2_N \quad EI/\rho A \tag{5}$$

Assuming a sinusoidal time response,

$$T_N(t) = C_1 \sin(\beta_N t) + C_2 \cos(\beta_N t) \tag{6}$$

C_1 and C_2 are determined by evaluating the initial conditions of the problem. At this point, each approach to analyzing the soft body impact must be treated separately.

1. INITIAL VELOCITY SOLUTION

The first approach taken was to assume the projectile imparts an initial velocity to the beam, as shown pictorially in Figure 11A. The velocity can be expressed as:

$$V = \bar{V}\delta(x - L) \tag{7}$$

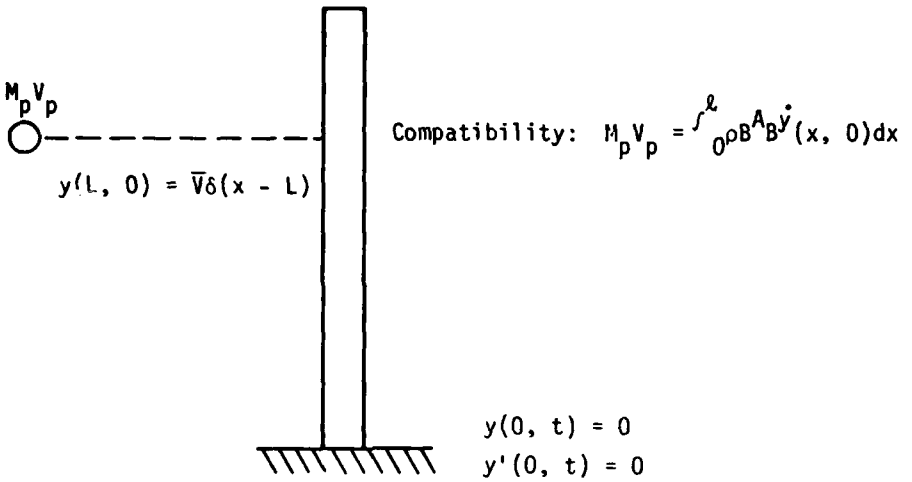

A) Initial Velocity at a Point

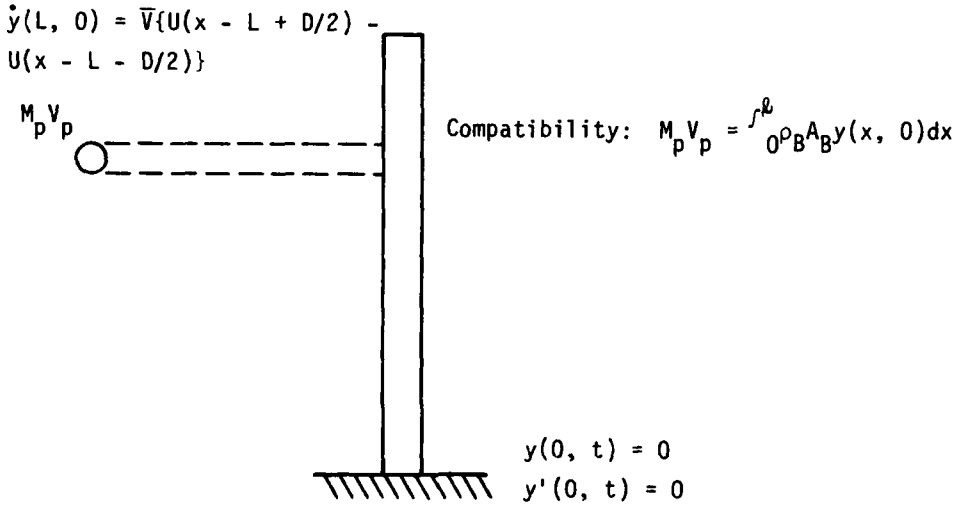

B) Initial Velocity Over an Area

Figure 11. Schematic of Initial Velocity Models

At time t = 0, the initial conditions are:

$$y(x, 0) = 0$$

$$\dot{y}(x, 0) = \bar{V}\delta(x - L)$$

Application of the I.C.s yields $C_2 = 0$ and

$$\bar{V}\ (x - L) = \sum_{N=1}^{\infty} A_N \omega_N \phi_N(x) \tag{8}$$

Multiplying both sides by a particular mode shape, $\phi_M(x)$, applying orthogonality conditions and integrating over the length of the beam results in:

$$\int_0^{\ell} \bar{V}\delta(x - L)\phi_M(x)dx = A_M\omega_M \int_0^{\ell} \phi_M^2(x)dx \tag{9}$$

The left hand side of Equation 9 reduces to $\bar{V}\phi_M(L)$, while the integral on the right hand side, when evaluated, equals ℓ (Reference 10). Therefore,

$$\bar{V} = A_M\omega_M\ell/\phi_M(L)$$

which leads to the solution for A_N,

$$A_N = A_1(\omega_1/\omega_N)[\phi_N(L)/\phi_1(L)] \tag{10}$$

A_1 must now be solved for to determine the complete solution. The relationship remaining is conservation of momentum. Applying this principle as previously described, the projectile momentum is equated to the net momentum of the beam. Thus,

$$M_pV_p = \int_0^{\ell} \rho_B A_B \dot{y}(x, t)dx$$

$$M_pV_p = \rho_B A_B \sum_{N=1}^{\infty} A_N\omega_N \cos(\omega_N t) \int_0^{\ell} \phi_N(x)dx$$

Evaluating the integral and substituting Equation 10 for A_N, we have

$$M_pV_p = 2\rho_B A_B \sum_{N=1}^{\infty} [A_1\omega_1\phi_N(L)/\beta_N\phi_1(L)]K_N \cos(\omega_N t)$$

where K_N is defined in Equation 3a. This relationship exists only at $t = 0$, therefore,

$$M_p V_p = 2M_B A_1 \omega_1 / \ell \phi_1(L) \sum_{N=1}^{\infty} \phi_N(L) K_N / \beta_N$$

Defining $C_S = \sum_{N=1}^{\infty} 2\phi_N(L) K_N / \beta_N \ell$ and solving for A_1,

$$A_1 = M_p V_p \phi_1(L) / M_B \omega_1 C_S$$

Thus, one can solve for A_N by substituting into Equation 10.

$$A_N = M_p V_p \phi_N(L) / M_B \omega_N C_S \tag{11}$$

The beam response to impact can now be written as:

$$y(x, t) = M_p V_p / M_B C_S \sum_{N=1}^{\infty} [\phi_N(L) / \omega_N] \phi_N(x) \cos(\omega_N t) \tag{12}$$

This solution can be further modified to simulate the projectile impact by spreading the initial velocity out from a point to an area, shown in Figure 11B. Equation 7 is rewritten as:

$$V = \bar{V}\{U[x - (L - D_p/2)] - U[x - (L + D_p/2)]\} \tag{13}$$

which spreads the impact over an area as wide as the projectile and euqally distributes it on either side of the impact span. The left hand side of Equation 9 now becomes:

$$\int_0^{\ell} \bar{V}\{U[x - (L - D_p/2)] - U[x - (L + D_p/2)]\} \phi_M(x) dx$$

which reduces to:

$$\bar{V} \int_{L - D_p/2}^{L + D_p/2} \phi_M(x) dx$$

Following through the solution, the final expression for the beam response becomes:

$$y(x, t) = M_p V_p / M_B C'_S \sum_{N=1}^{\infty} [\phi^1_N / \omega_N] \phi_N(x) \cos(\omega_N t) \tag{14}$$

where

$$\phi_N^1 = \int_{L - D_p/2}^{L + D_p/2} \phi(x)dx \tag{15}$$

and

$$C'_S = \sum_{N=1}^{\infty} 2K_N \phi^1_N / \beta_N \ell \tag{16}$$

Both solutions, for impact at a point and over an area, were programmed on the computer to be evaluated against test data.

2. FORCED VIBRATION

The second approach taken was to treat the impact as a forced vibration problem for the duration of projectile contact, shown in Figure 12A. The solution to such a problem is in two parts, the homogeneous (free vibration) solution and the particular (forced vibration) solution. The homogeneous solution is that given in Equation 4. The particular solution is developed below.

First, the forcing function was assumed to be a constant force at a point acting over a finite time period. In other words,

$$F(x, t) = \bar{F}\delta(x - L)[U(t) - U(t - T_0)] \tag{17}$$

The time interval, T_0, over which the force acts is determined in Reference 7 to be the time necessary for the projectile to traverse its diameter, or

$$T_0 = D_p/V_p$$

The beam mode shape meets all special requirements of the differential equation, independent of time. Therefore, the assumed particular solution is:

$$y_p(x, t) = \sum_{N=1}^{\infty} A_N \phi_N(x) T_N(t)$$

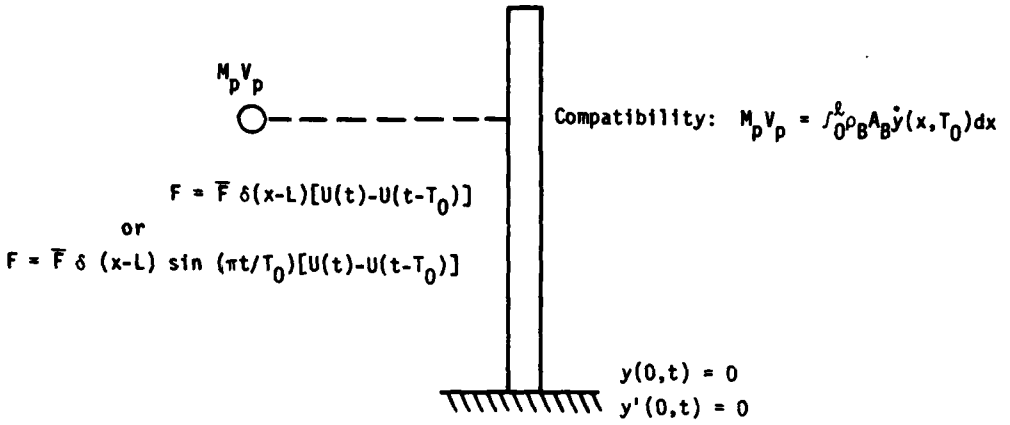

A) Forced Vibration At A Point

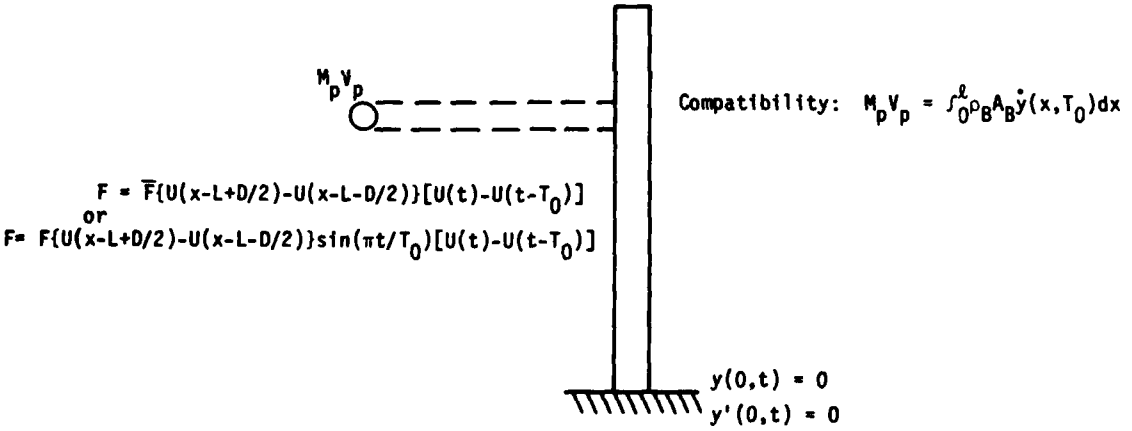

B) Forced Vibration Over An Area

Figure 12. Schematic of Forced Vibration Models

Substituting this into the beam equation, we have

$$\sum_{N=1}^{\infty} \beta_N^4 A_N \phi_N(x) T_N(t) - \rho_B A_B / EI_N \sum_{1}^{\infty} A_N \phi_N(x) \ddot{T}_N(t) =$$

$$\bar{F}\delta(x - L)[U(t) - U(t - T_0)]/EI\ell$$

Applying orthogonality, as before, this expression reduces to,

$$\beta_M^4 A_M \ell T_M(t) - (\rho_B A_B \ell / EI)\ddot{T}_M(t) = (\bar{F}\phi_M(L)/EI\ell)[U(t) - U(t - T_0)] \tag{18}$$

For all time except between $t = 0$ and $t = T_0$, the right hand side of Equation 18 is zero, thus $T_M(t)$ is zero for the same time. For $0 \leq t \leq T_0$, the right hand side of Equation 18 is a constant, therefore, $T_M(t)$ is a constant and the equation reduces to

$$\beta_M \ell C_M = \bar{F}\phi_M(L)/EI\ell$$

which further reduces to an expression for C_M,

$$C_M = \bar{F}\phi_M(L)/\rho_B A_B \omega_M \ell \tag{19}$$

This is the particular solution to the differential equation which, when combined with the homogeneous solution, leads to the total solution to the forced vibration problem,

$$y_T(x, t) = \sum_{N=1}^{\infty} [A_N \sin(\omega_N t) + B_N \cos(\omega_N t) + C_N]\phi_N(x) \tag{20}$$

Evaluating the initial conditions, $y(x, 0) = \dot{y}(x, 0) = 0$, leads to

$$y_T(x, t) = \sum_{N=1}^{\infty} C_N[1 - \cos(\omega_N t)]\phi_N(x) \tag{21}$$

This solution is valid for $0 \leq t \leq T_0$, at which time the force is removed and the problem becomes free vibration with deflection and velocity initial conditions from the forced response. Evaluating and applying these initial conditions results in two equations and two unknowns which provides expressions for A_N and B_N. The solution for $t \geq T_0$ is then,

$$y_F^1(x, t) = \sum_{N=1}^{\infty} C_N\{\sin(\omega_N T_0)\sin(\omega_N t) - [1 - \cos(\omega_N T_0)]$$

$$\cos(\omega_N t)\}\phi_N(x) \qquad (22)$$

The only unknown at this point is $\overline{F}$, which can be determined from the conservation of linear momentum assumption. Projectile and beam momentum are formulated in the same manner as in the initial velocity analysis, with the additional requirement that the transfer is complete at time T_0. From this, $\overline{F}$ is determined to be

$$\overline{F} = M_p V_p \ell / C_S^F$$

where

$$C_S^F = \sum_{N=1}^{\infty} (2\phi_N(L) K_N / \omega_N \beta_N \ell)\sin(\omega_N T_0)$$

Hence, C_N is

$$C_N = M_p V_p \phi_N(L) / M_B \omega_N^2 C_S^F \qquad (23)$$

The forced vibration solution becomes

$$y_T(x, t) = (M_p V_p / M_B C_S^F)_N \sum_{N=1}^{\infty} (\phi_N(L)/\omega_N^2)[1 - \cos(\omega_N t)]\phi_N(x)$$

$$\text{for } 0 \leq t \leq T_0 \qquad (24)$$

and the free vibration solution becomes

$$y_F^1(x, t) = (M_p V_p / M_B C_S^F)_N \sum_{N=1}^{\infty} (\phi_N(L)/\omega_N^2)\{\sin(\omega_N T_0)\sin(\omega_N t) -$$

$$[1 - \cos(\omega_N T_0)]\cos(\omega_N t)\}\phi_N(x) \text{ for } t \geq T_0 \qquad (25)$$

This solution can also be modified, as was the initial velocity solution, to spread the force over an area as wide as the projectile, as shown in Figure 12B. The analysis procedure is the same as before and results in the same solutions as Equations 24 and 25 with two

substitutions. $\phi_N(L)$ is replaced by $\phi_N^1(L) = \int_{L - D_p/2}^{L + D_p/2} \phi_N(x)dx$ and C_S^F is replaced by $C_S^{F'} = \sum_{N=1}^{\infty}(2\phi_N^1(L)K_N/\omega_N\beta_N\ell)\sin\omega_N T_0$.

A second set of solutions can be obtained by assuming the forcing function to be a half-sine wave, as opposed to a square wave, acting over the impact duration. This assumption makes the force take the form, also shown schematically in Figure 12A,

$$F(x, t) = \bar{F}\delta(x - L)\sin(\pi t/T_0)[U(t) - U(t - T_0)]$$

and Equation 18 becomes

$$\beta_M^4 A_M \ell T_M(t) - (\rho_B A_B \ell/EI)\ddot{T}_M(t) = [\bar{F}\phi_M(L)/EI\ell]\sin(\pi t/T_0) \qquad (26)$$

Letting $T_M(t) = R_M\sin(\pi t/T_0)$, differentiating, and substituting into Equation 26 results in the equation

$$EI\beta_M^4\ell R_M + (\pi^2\rho_B A_B\ell/T_0^2)R_M = \bar{F}\phi_M(1)/\ell$$

which, when reduced and solved for R_M, yields

$$R_M = \bar{F}\phi_M(L)/M_B(\omega_M^2 + \pi^2/T_0^2)\ell \qquad (27)$$

This expression is substituted in Equation 20 and solved with initial conditions for A_N and B_N to give the total forced response as

$$y_F(x, t) = \sum_{N=1}^{\infty} R_N[\sin(\pi t/T_0) - (\pi/T_0\omega_N)\sin(\omega_N t)]\phi_N(x) \qquad (28)$$

As before, Equation 28 is used to develop initial conditions at $t = T_0$ for the free vibration solution for $t \geq T_0$. This solution is

$$y_F^1(x, t) = \sum_{N=1}^{\infty}(-\pi R_N/T_0\omega_N)[1 + \cos\omega_N T_0)\sin(\omega_N t) - \sin(\omega_N T_0)\cos(\omega_N t)]\phi_N(x) \qquad (29)$$

The conservation of momentum yields

$$\overline{F} = (M_p D_p \ell/\pi C_S)$$

where

$$C_S = \sum_{N=1}^{\infty} 2K_N \phi_N(L)[1 + \cos(\omega_N T_0)]/\beta_N \ell(\omega_N^2 + \pi^2/T_0^2)$$

Thus, R_N is given as

$$R_N = M_p D_p \phi_N(L)/\pi C_S M_B(\omega_N^2 + \pi^2/T_0^2) \tag{30}$$

which, in turn, results in the total response for $0 \leq t \leq T_0$ being

$$y_F(x, t) = (M_p D_p/\pi M_B C_S)_N \sum_{1}^{\infty} [\phi_N(L)(\omega_N^2 + \pi^2 T_0^2)][\sin(\pi t/T_0) - (\pi/T_0\omega_N)\sin(\omega_N t)]\phi_N(x) \tag{31}$$

and the response for $t \geq T_0$ being

$$y_F^1(x, t) = (-M_p V_p/M_B C_S)_N \sum_{1}^{\infty} [\phi_N(L)/\omega_N(\omega_N^2 + \pi^2/T_0^2)]$$

$$\{[1 + \cos(\omega_N T_0)]\sin(\omega_N t) - \sin(\omega_N T_0)\cos(\omega_N t)\}\phi_N(x)$$

A solution for the half-sine wave spread over an area as depicted in Figure 12B can be obtained by making the substitution of $\int_{L - D_p/2}^{L + D_p/2} \phi_N(x)dx$ for $\phi_N(L)$ in the appropriate places in Equations 31 and 32.

All the aforementioned solutions for forced vibration at a point (Equations 24, 25, 31, 32) and also those for forced vibration over an area were converted to computer programs for evaluation against test data.

SECTION IV

NUMERICAL ANALYSIS AND RESULTS

Each theoretical solution derived was programmed for analysis on the digital computer. The program was written for use at an interactive graphics terminal so that several parameters in any particular problem could be easily varied and results compared. The required input included beam parameters (dimensions, material properties), projectile parameters (diameter, density, velocity), the number of modes to be used in the summation, and the time period over which to make strain calculations. Damping effects could be included, at the user's option. When included, damping was modeled by decaying exponential functions applied to each mode. The values of ξ included in the program were based on actual damping measurements taken from each test specimen.

Initially, numerical difficulty was encountered evaluating sinh and cosh functions for large values of β. The problem arose in calculating K in Equation 3a and stemmed from taking small differences of large numbers. As β increased, so did the values of sinh and cosh until the accuracy of the computer was exceeded. The problem was solved by expressing hyperbolic functions in the mode shape equation as exponentials. A complete derivation of the expressions used to calculate $\phi(x)$ is included in Appendix D. Once the exponential equations were included, all numerical problems were corrected and accurate solutions were obtained from the program, which are listed in Appendix E.

Results calculated and included in the output were the maximum absolute value of strain calculated over the specified time period, the time at which it occurred, the resonant frequency of each mode used in the summation, and, if desired, a plot of strain versus time. Figure 13 is an example of the program input and output and Figure 14 exemplifies the type of strain/time plot generated. The program was used to calculate theoretical impact responses for comparison with each other and with experimental results.

```
MODEL OPTIONS ARE-

        POINT I.C.-INITIAL VELOCITY AT A POINT
        AREA I.C.-INITIAL VELOCITY OVER AN AREA
        FORCED VIBRATION AT A POINT
        FORCED VIBRATION OVER AN AREA
        END
OPTION-FV
DO YOU WANT DAMPING?-Y
HOW MANY MODES DO YOU WANT TO USE ? -5
ENTER THE DIMENSIONS, DENSITY, AND MODULUS OF YOUR BEAM.
L,W,T,RHO,AND E -5.6,1.2,.15,.101,1.04E7
ENTER IMPACT POINT AND POINT FOR STRAIN CALCS IN % OF L -75,75
ENTER DIAMETER, DENSITY, AND VELOCITY OF THE PROJECTILE -.5,.0316,341
WHAT TIME PERIOD DO YOU WANT TO CALCULATE STRAIN OVER?(500, 50, 5, OR
 0.5 MS.) -50
 THE MAX STRAIN IS  .1050202-02 OCCURRING AT  .750000E-03 SECONDS.
      MODE    FREQUENCY, HZ.     COEFFICIENT     DIA,IN.     VEL, F/S
      1         .154044E+03       .7178955E+00   .500E+00   .341E+03
      2         .965379E+03       .375127E-02    .500E+00   .341E+03
      3         .270309E+04      -.2031047E-02   .500E+00   .341E+03
      4         .529599E+04       .5706315E-03   .500E+00   .341E+03
      5         .875828E+04      -.8047438E-04   .500E+00   .341E+03
PLOT? -Y
```

Figure 13. Example of Computer Input/Output

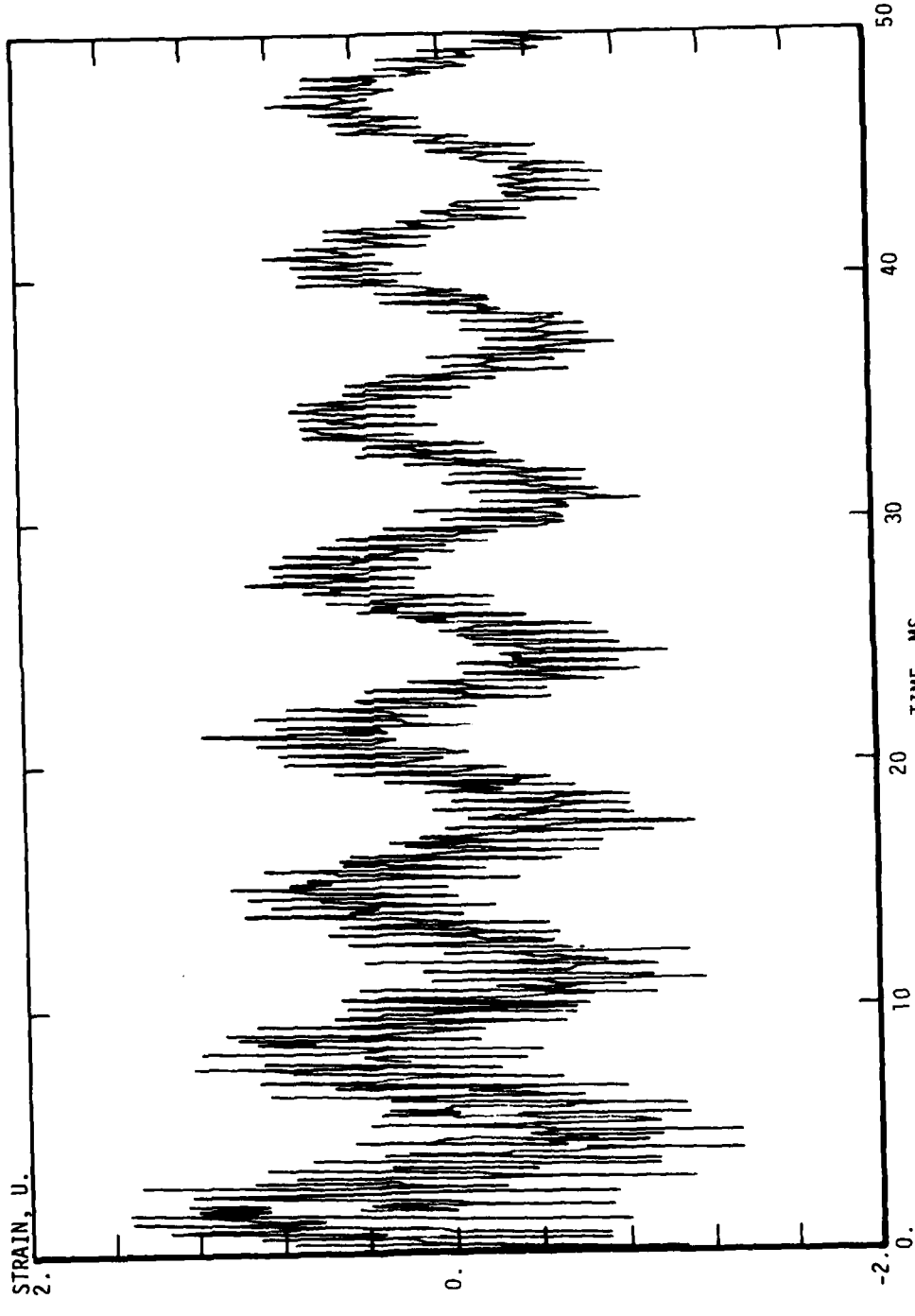

Figure 14. Example of Computer Generated Strain vs. Time Plot

Table 2 contains values of maximum strain calculated by each model at the root of a particular beam. The number of modes used in each model was varied to determine how many were necessary for the strain value to stabilize. It is apparent that the point initial velocity solution does not stabilize, i.e., the more modes included in the solution, the higher the calculated value of strain. Spreading the initial velocity over an area decreased the rate at which strain increased, but did not stabilize the solution. Both forced vibration models which treat the force as a square wave stabilize at five modes, with addition of more changing the max strain value less than 4%. The half-sine wave models also stabilize at five modes with less than 2% variation in the max strain value thereafter. Table 3 shows the effect of damping on the maximum strain values. The values calculated by the point and area initial condition models decrease by 24% and 19%, respectively. Values of strain from both square wave forced vibration models decreased 2% while the half-sine wave models predicted strain 6% lower than those with no damping.

These results lead to two conclusions concerning the theoretical models. First, the initial velocity solutions, although shown in Reference 3 to simulate hard-body impacts, do not provide reasonable simulations of the soft-body problem. The non-converging strain values calculated by both are not realistic. For this reason, these models will not be considered in test data comparisons. Second, all forced vibration solutions appear to provide reasonable results and should be further evaluated and compared to test data to verify the validity of each.

TABLE 2

THEORETICAL RESULTS WITHOUT DAMPING*

5.6 INCH BEAM; ρ_p = 0.032 lbm/in^3; D_p = 0.5; V_p = 340 f/s

Number of Modes	ϵ_{root},%					
	PIC	AIC	FV	FA	FV'	FA'
1	0.186	0.118	0.187	0.187	0.187	0.187
2	0.149	0.091	0.150	0.150	0.201	0.201
3	0.328	0.182	0.267	0.264	0.266	0.264
4	0.400	0.214	0.329	0.323	0.287	0.284
5	0.458	0.241	0.327	0.321	0.292	0.289
10	0.578	0.285	0.339	0.330	0.288	0.284
20	0.990	0.348	0.340	0.332	0.287	0.284

PIC = Initial Velocity at a Point
AIC = Initial Velocity Over an Area
FV = Forced Vibration at a Point; Step-Function Model
FA = Forced Vibration Over an Area; Step-Function Model
FV' = Forced Vibration at a Point; Half-Sine Wave Model
FA' = Forced Vibration Over an Area; Half-Sine Wave Model

* Strains are absolute value

TABLE 3

THEORETICAL RESULTS WITH DAMPING*

5.6 INCH BEAM; ρ_p = 0.032 lbm/in ; D_p = 0.5; V_p = 340 f/s

Number of Modes	ε_{root},%					
	PIC	AIC	FV	FA	FV'	FA'
10	0.438	0.230	0.331	0.323	0.270	0.267

* Strains are absolute value

SECTION V

COMPARISON OF EXPERIMENTAL AND THEORETICAL RESULTS

Table 4 shows the maximum root strain from one of each size test beam and the predicted values from each forced vibration model. The percentage differences between the predicted and experimental values indicate that forced vibration with a half-sine wave force over an area provides the best correlation without damping effects included, although the half-sine wave force at a point is only slightly different. Predicted results for the 5.6 inch beam are significantly higher than the experimental ones due to damping effects in the third and fourth modes which were not accounted for in the analytical predictions. If some reasonable values of damping are included in the predictions, the percent error is decreased to that shown in Table 5.

The results in Table 2 indicate that in all the forced vibration models, the entire response can be simulated using only the first four modes. This agrees with the Fourier transform plots in Figure 9. Predictions of strain from the same models show that this is also true at 75% span, which agrees with Figure 10.

The differences between predictions applying the force at a point and over an area are less than 2%. This difference is small enough that results from either model are acceptable.

Figures 15A and 15B are plots of predicted strain response from both the step function and half-sine wave models at the 5.6 inch beam root. These can be compared to Figure 4A. Both models predict the same basic response shape as that determined from experiments over the 50 millisecond interval.

Comparison of Figures 16A and 17A to the experimental short time response in Figure 6A shows that the step function model predicts beam response more accurately than the half sine wave model does. Further comparison of Figures 16B through 16D to Figures 6B through 6D reconfirms the step function model accuracy. For final verification, Figures 18A through 18D can be compared to Figures 7A through 7D, which firmly verifies this model.

Investigation of the half-sine wave model shows that it predicts the same basic response shape as the experiments, but the higher frequency (3rd and 4th) modes are apparently not accounted for correctly. Response plots from this model are shown in Figures 17A through 17D for comparison with Figures 6A through 6D.

TABLE 4

COMPARISON OF EXPERIMENTAL AND THEORETICAL RESULTS*

Beam Length, in.; ρ_p,lbm/in^3; V_p,f/s	Experimental ε_{root},%	FV		FA		FV'		FA'	
		ε_r,%	Δ,%	ε_r,%	Δ,%	ε_r,%	Δ,%	ε_r,%	Δ,%
5.6;.031;370	0.278	0.368	32.4	0.360	29.5	0.326	17.3	0.322	15.8
8.4;.0307;344	0.231	0.272	17.7	0.267	15.6	0.250	8.2	0.247	6.9
11.2;.0303;366	0.282	0.353	25.2	0.346	22.7	0.312	10.6	0.308	9.2
14.0;.033;317	0.254	0.302	18.9	0.297	16.9	0.272	7.1	0.269	5.9

* Strains are absolute value; theoretical results do not include damping

TABLE 5

COMPARISON OF EXPERIMENTAL AND THEORETICAL RESULTS WITH DAMPING

Beam Length, in; ρ_p,lbm/in^3; V_p,f/s	Experimental ε_{root},%	FV		FA		FV'		FA'	
		ε_r,%	Δ,%	ε_r,%	Δ,%	ε_r,%	Δ,%	ε_r,%	Δ,%
5.6;0.031;370	0.278	0.303	9.0	0.297	6.8	0.252	-9.4	0.250	-10.0

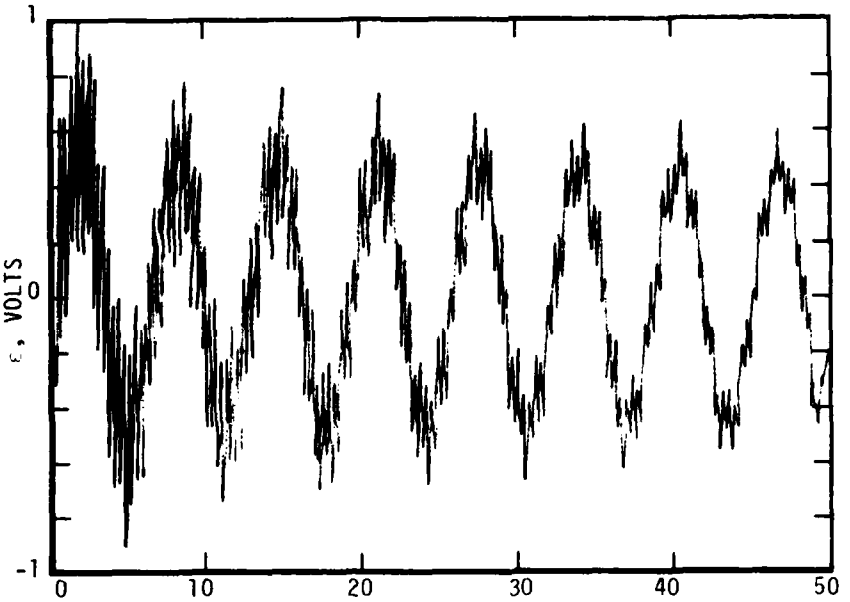

A) Step-Function Model

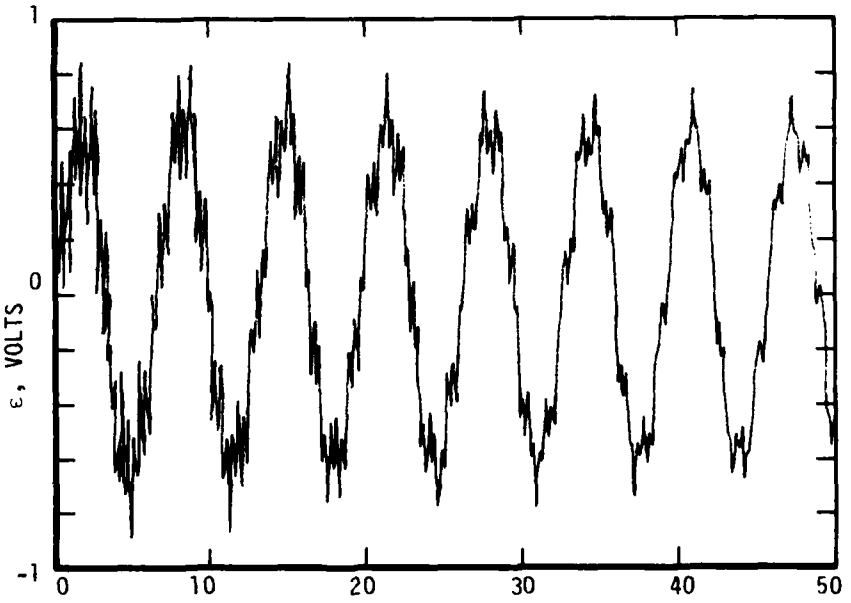

B) Half-Sine Wave Model

Figure 15. Strain at Root of 5.6 Inch Beam From Forced Vibration Models

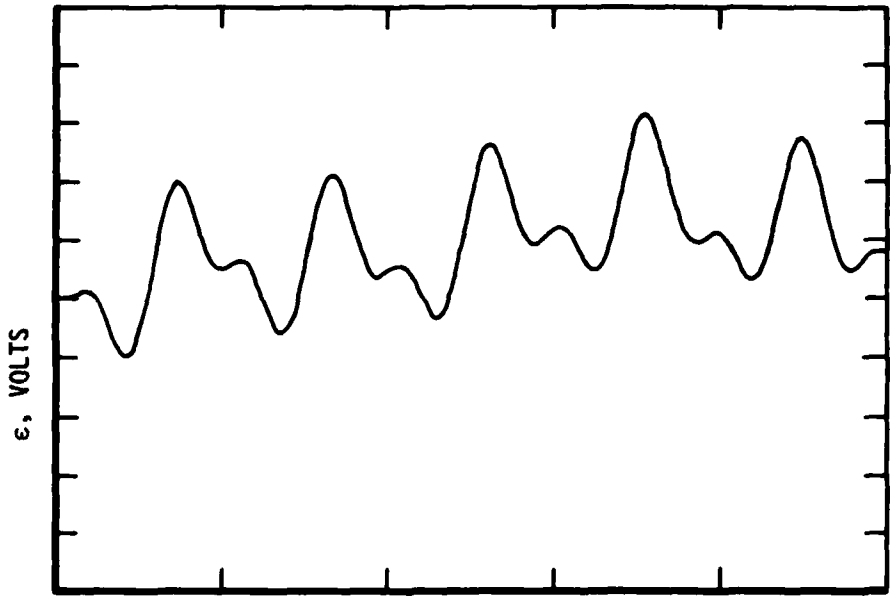

A) Root Location

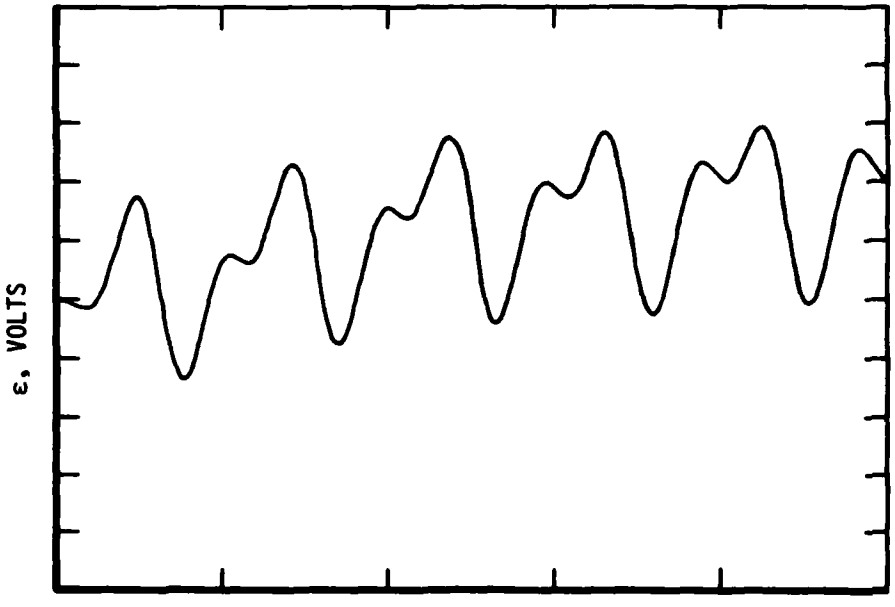

B) 25% Span

Figure 16. Strain in 14.0 Inch Beam From Step Function Model (5.0 ms.)

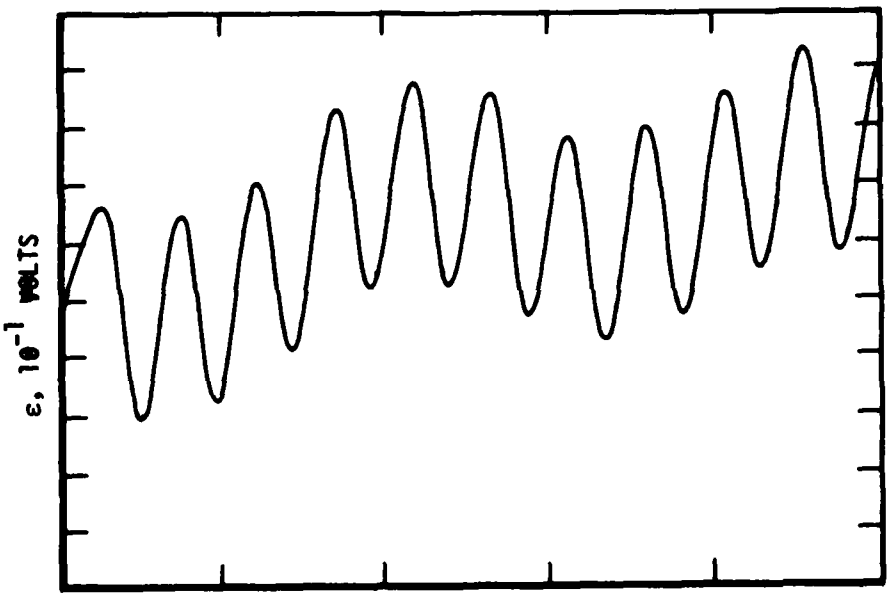

C) 50% Span

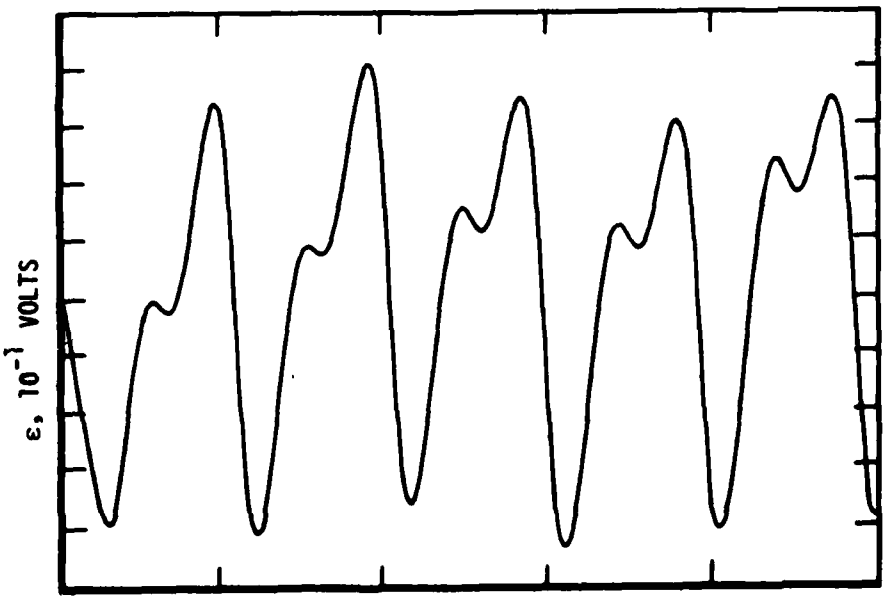

D) 75% Span

Figure 16. (Contd)

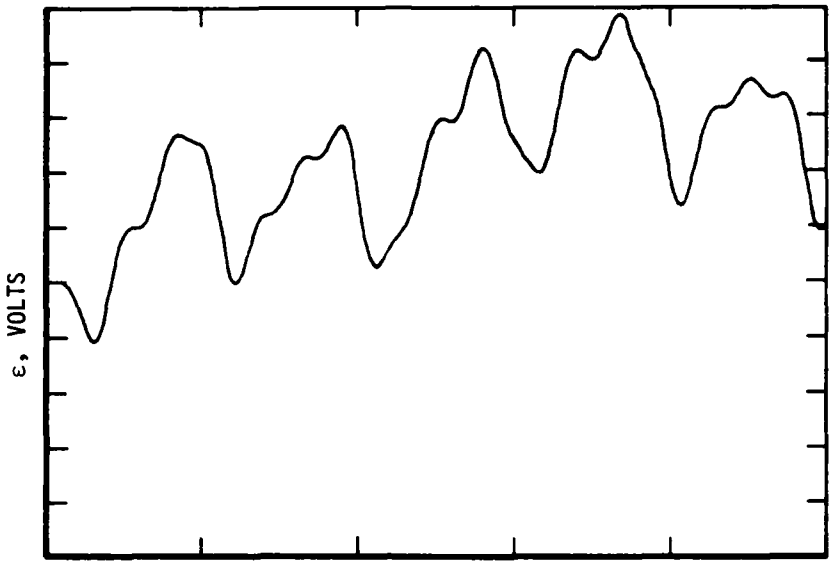

A) Root Location

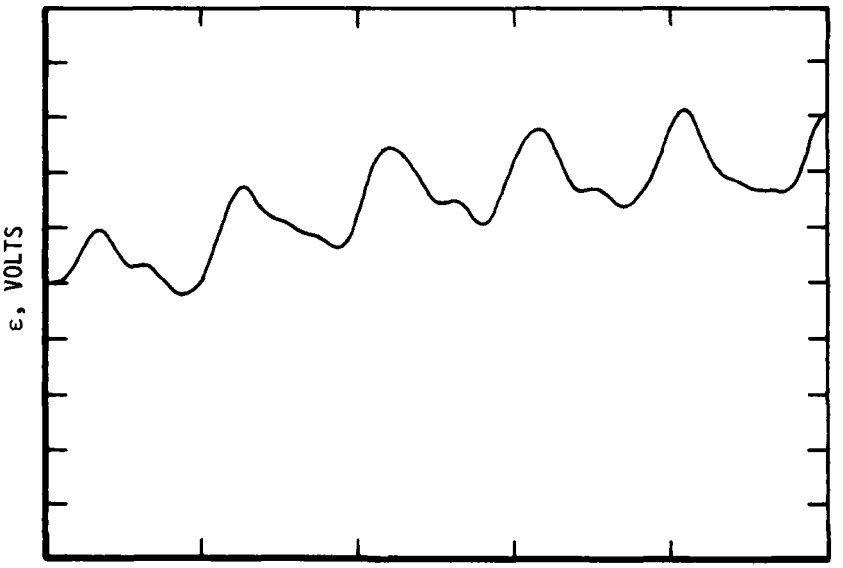

B) 25% Span

Figure 17. Strain in 14.0 Inch Beam From Half-Sine Wave Model (5.0 ms.)

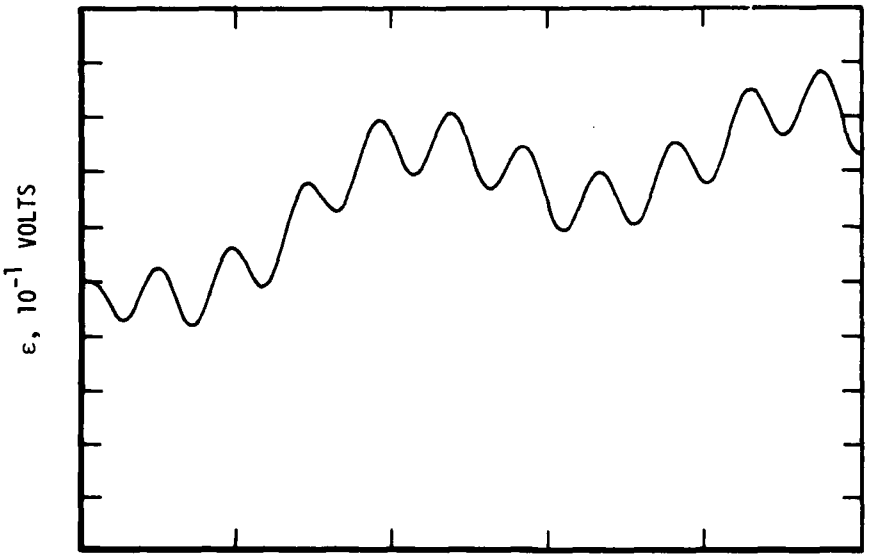

C) 50% Span

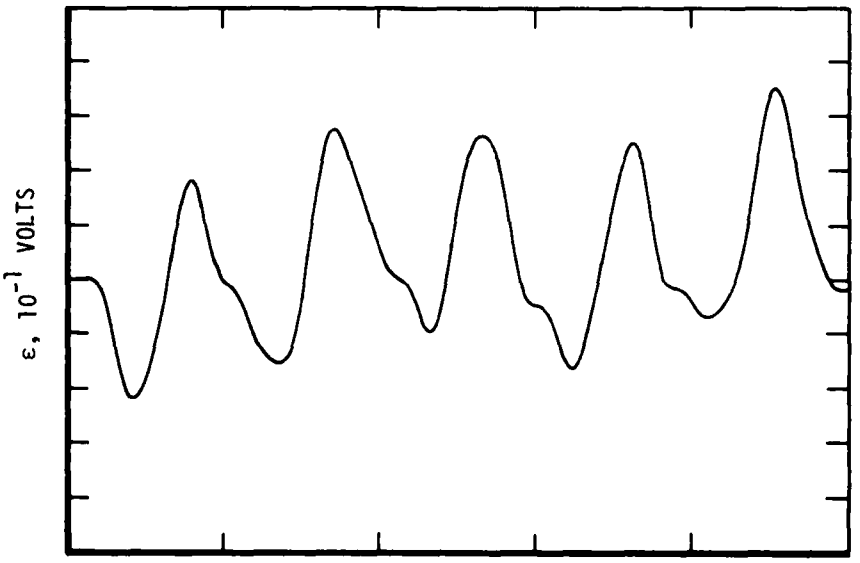

D) 75% Span

Figure 17. (Contd)

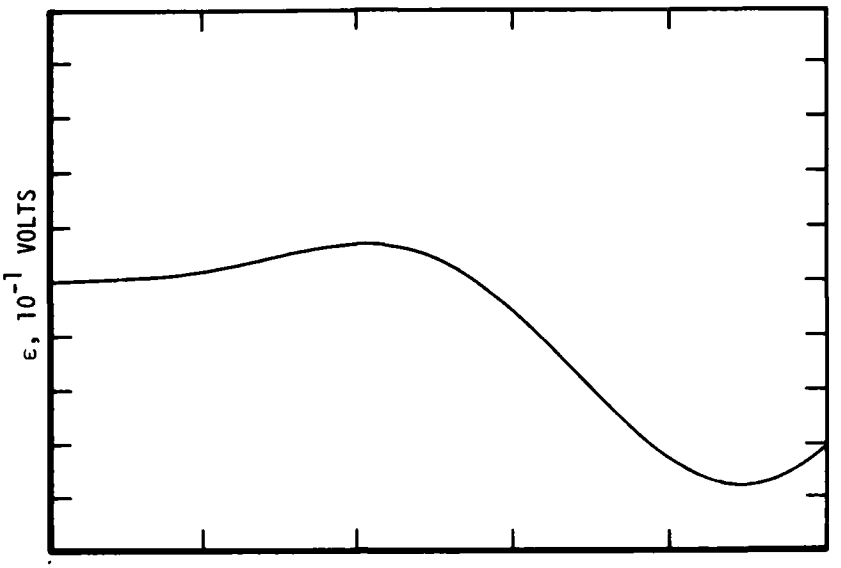

A) Root Location

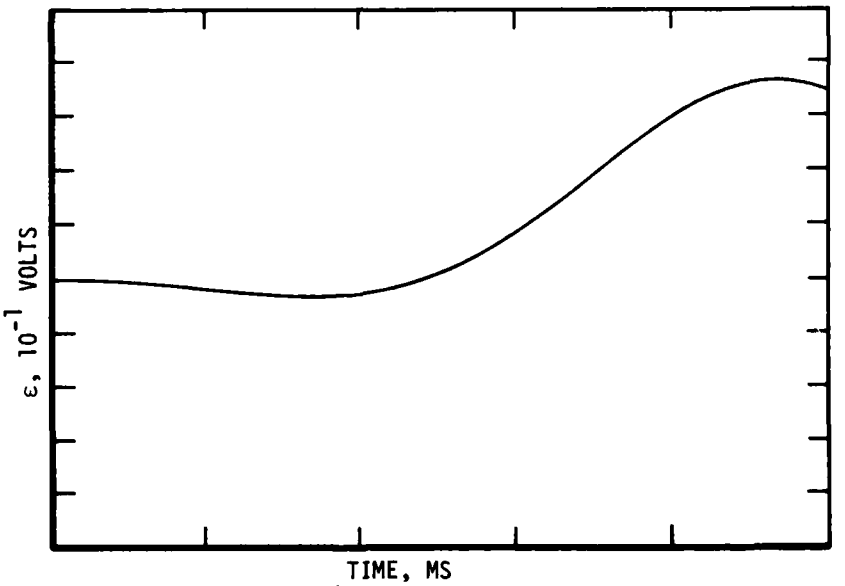

B) 25% Span

Figure 18. Strain in 14.0 Inch Beam From Step Function Model (0.5 ms.)

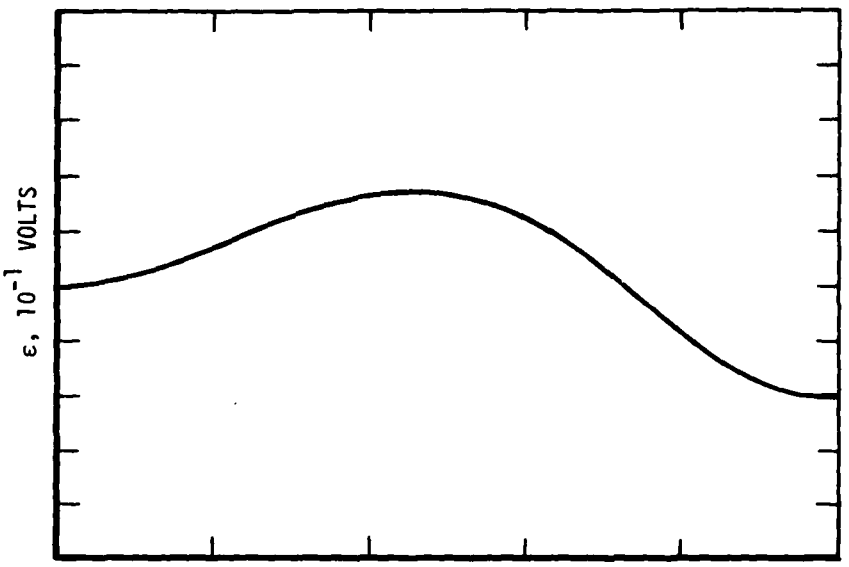

C) 50% SPAN

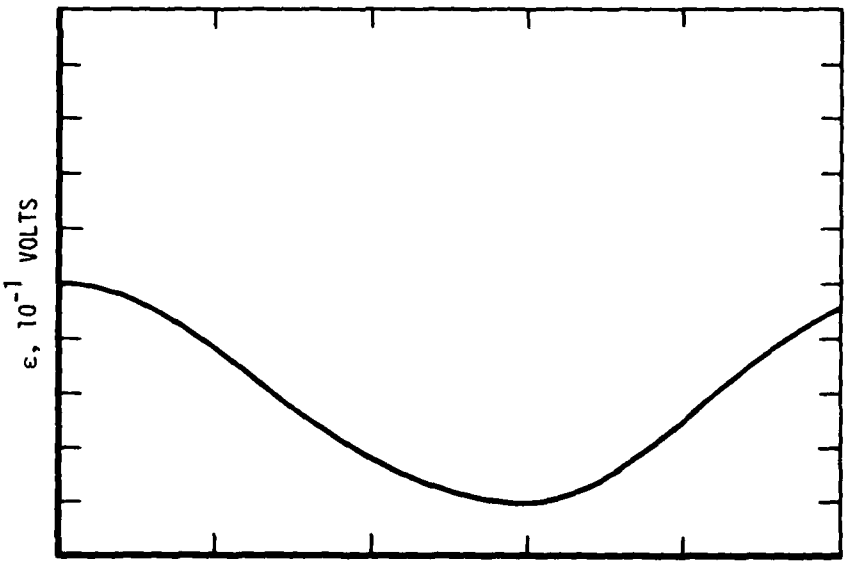

D) 75% SPAN

Figure 18. (Cont'd)

SECTION VI

DISCUSSION AND CONCLUSION

The experimental data provided an excellent base from which to evaluate theoretical models. Both the FFT system and the high speed transient recorder proved to be very valuable tools for studying the impact problem. Fourier transforms of test data made it immediately apparent that the initial velocity solutions were not adequate models. Also, the very short-time response plots from the transient recorder dispelled any questions of high frequency bending waves causing responses the FFT system could not record.

Both the strain values and graphic displays of beam response data allowed complete verification of the step function forced vibration model. Correlation between actual data plots and the predicted response was surprising and proved to be the discerning factor between the step function and half-sine wave formulations. The only question that might arise would be why the half-sine wave model more closely predicts maximum strain. The answer to this may be in the damping present in the beam/fixture system. Accurate modal damping values could not be obtained while the beams were mounted on the impact range; thus, any values employed in the models were approximate. Conceivably, if the actual ξ values for each mode could be modeled into the computer simulation, values of strain predicted would be much closer to experimental values. Additional damping could also enter the system through the projectile/beam interface. Plastic flow and many other undefined phenomena taking place in the projectile during impact could cause small reductions in beam response.

The beams tested were specifically chosen to approximate the stiffness of typical jet engine fan blades. Timoshenko effects were negligible in this base because high order modes did not lend any significant contributions to beam response. For beams of different geometric properties where λ/t (modal wave length/beam thickness) reaches ten in the first several modes, the impact problem requires Timoshenko beam theory to account for shear and rotary inertia. However, as long

as λ/t is greater than ten, an Euler-Bernoulli beam theory formulation, which models soft-body impact as a forced vibration, treats the impact as a step function force in time and assumes a complete momentum transfer from projectile to beam will provide a good solution for elastic beam response. The accuracy of results from such a model is good for short-time response and can be improved for long-time response by addition of damping effects. Future work in this area can build upon this basis and the fact that linearly scaled beams and projectiles will produce equal strains. This means that the response of very large beam-like structures to soft-body impacts can be determined from analysis or testing of scaled-down models and the results will not require scaling.

APPENDIX A - ESTIMATION OF PROJECTILE VELOCITY

According to Reference 6, the stress at the beam root is

$$\sigma_{root} = KAXh/2I_0$$

where

$X \equiv$ Impact Location

$h \equiv$ Beam Thickness

$I_0 \equiv$ Minimum Area Moment of Inertia

The values of X, h, and I_0 are determined directly from the particular beam geometry. K is the equivalent beam stiffness determined from Figure 5, Reference 6 as a function of impact site. A is the effective first mode amplitude at the impact site. For a strain of 0.25%, σ_{root} is 25,000 psi which gives A as

$$A = (50,000)I_0/XKh$$

For the 8.4 inch beam,

$$A = (50,000)\ (0.0017086)/(6.3)\ (202)\ (.225) = 0.299 \text{ in.}$$

Assuming simusoidal motion,

$$V = A\omega$$

where ω is the effective first mode frequency, determined from

$$\omega = K/M$$

M is obtained from Figure 6, Reference 6. Thus, we have

$$\omega = 202 \times 386/.227 = 586 \text{ HZ}$$

Thus, the velocity is

$$V = A\omega = 175 \text{ in/s}$$

Assuming complete momentum transfer from the projectile to the beam, the projectile velocity can be approximated by

$$V_p = V_B M/M_p$$

The projectile material density is typically 0.033 lbm/in^3, and the diameter for this case is 0.7 inches, therefore,

$$V_p = (175) \times (0.227)/(0.00584) = 6800 \text{ in/s}$$

or

$$V_p = 570 \text{ f/s}$$

APPENDIX B - STRAIN IN LINEARLY SCALED BEAMS

The elementary formula for bending strain in a beam is:

$$\varepsilon = Mc/IE$$

$M \equiv$ Bending Moment

$c \equiv$ Distance from Neutral Bending Axis

$I \equiv$ Moment of Inertia of Beam Cross-Section

$E \equiv$ Young's Modulus

For two linearly scaled beams,

$$I_1 = wt^3/12 \qquad I_2 = (K)w(K^3)t^3/12 = K^4 I_1$$

and

$$c_2 = Kc_1$$

Therefore,

$$\varepsilon_1 = M_1 c_1 / I_1 E$$

and

$$\varepsilon_2 = M_2 K c_1 / K^4 I_1 E = (1/K^3) M_2 c_1 / I_1 E$$

The bending moment, M, is created by a force that is proportional to the momentum of the projectile.

$$\int_0^{T_0} F dt \simeq m_p V_p \rightarrow F \simeq m_p V_p / T_0$$

$m_p \equiv$ Projectile Mass

$V_p \equiv$ Projectile Velocity

$T_0 \equiv$ Duration of Impact

For linearly scaled projectiles and equal projectile velocities,

$$m_{p1} = \rho\pi D_1^3/8 \qquad \text{and} \qquad m_{p2} = K^3\rho\pi D_1^3/8 = K^3 m_{p1}$$

$$T_{0_1} = D_1/V_p \qquad \text{and} \qquad T_{0_2} = K(D_1/V_p) = KT_{0_1}$$

Therefore,

$$F_1 \simeq m_{p1}V_p/T_{0_1} \qquad \text{and} \qquad F_2 \simeq K^3 m_{p1}V_p/KT_{0_1} = K^2F_1$$

The moment arm in each case, L, is also linearly scaled so that the bending moments are

$$M_1 = F_1 \times L_1 \qquad \text{and} \qquad M_2 = K^2F_1KL_1 = K^3M_1$$

The bending strain is now

$$\varepsilon_1 = M_1c_1/I_1E \qquad \text{and} \qquad \varepsilon_2 = (1/K^3)(K^3M_1c_1/I_1E) =$$

$$M_1c_1/I_1E$$

This shows that if the force created is proportional to the projectile momentum, equal strains will be created in linearly scaled beams impacted by linearly scaled projectiles (which is in agreement with experimental results observed).

APPENDIX C - EVALUATION OF TIMOSHENKO BEAM THEORY EFFECTS

When modes of vibration are considered in an analysis, the Euler-Bernoulli Beam Theory provides adequate eigenvalue predictions up to a certain point. When the effective wavelength of a particular mode is of the order of ten times the thickness of the beam being considered, shear effects start to become significant and the Timoshenko Theory is necessary to make adequate eigenvalue calculations. Figure C-1 is a plot of effective wavelength to thickness ratio versus mode number for a cantilever beam. This indicates that for the beams used in the impact experiments, shear effects will be negligible until the twentieth mode of the smallest beam. The lowest curve on Figure 16 represents a beam of thickness equal to one-fourth its length. Analysis of this class of geometries should employ the Timoshenko Theory to predict impact response accurately. Since only the first four or five modes were apparent in test data and the same number were necessary in theoretical predictions, the Euler-Bernoulli Theory is adequate to model the soft-body impact problem as considered in this analysis.

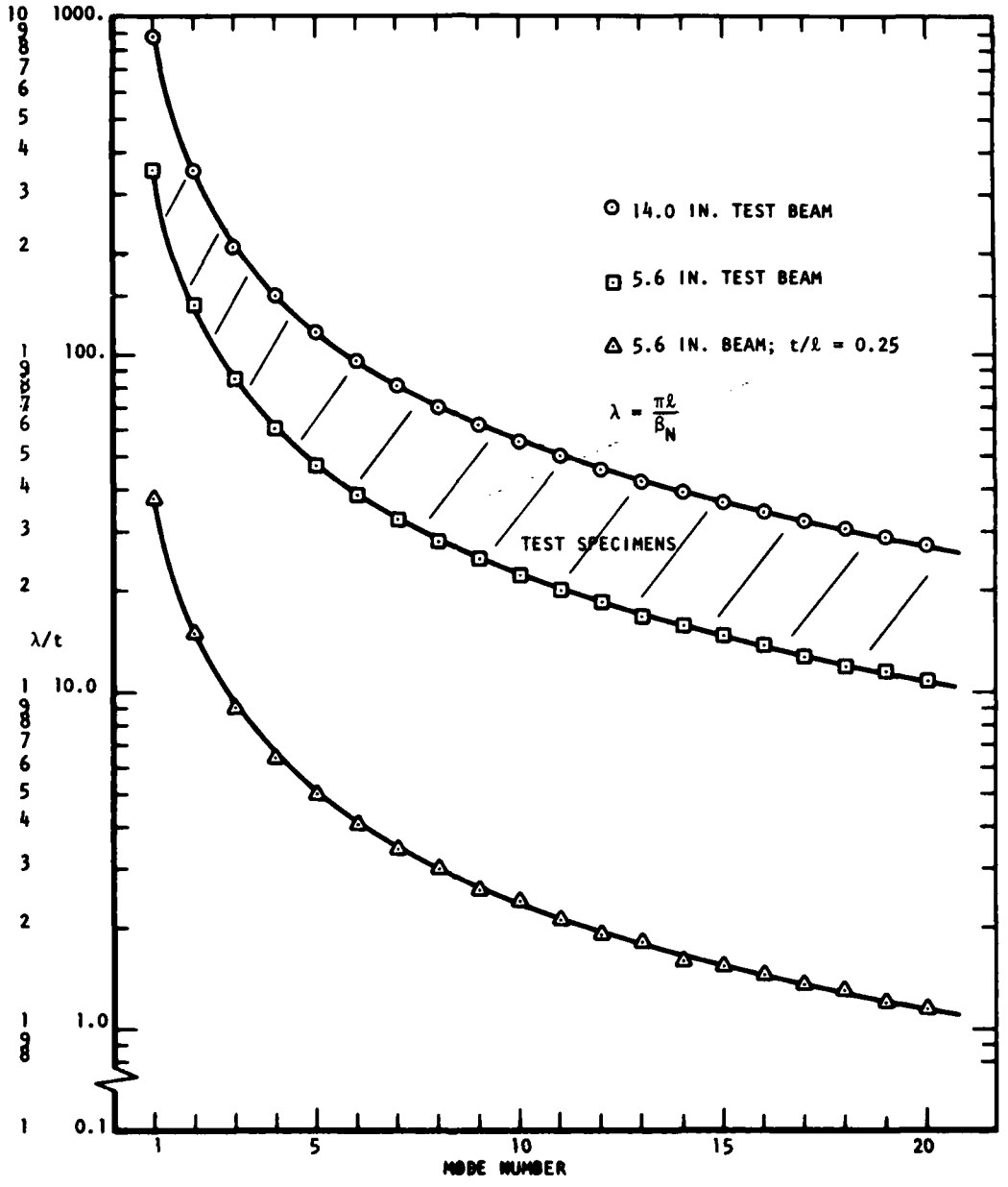

Figure C-1. Shear Effects in Cantilever Beam Vibration

APPENDIX D - NUMERICAL STABILITY

$$\phi_N(x) = \cosh(\beta_N x) - \cos(\beta_N x) - \{[\sinh(\beta_N \ell) - \sin(\beta_N \ell)]/$$

$$[\cosh(\beta_N \ell) + \cos(\beta_N \ell)]\}[\sinh(\beta_N x) - \sin(\beta_N x)]$$

To evaluate this expression on a computer, the hyperbolic functions must be expressed as exponentials. This leads to

$$\phi_N(x) = (1/2)e^{\beta_N x}(1 - K_N) + (1/2)e^{-\beta_N x}(1 + K_N) - \cos(\beta_N x) +$$

$$K_N \sin(\beta_N x)$$

where

$$K_N = [e^{\beta_N \ell} - e^{-\beta_N \ell}/2 - \sin(\beta_N \ell)]/[e^{\beta_N \ell} + e^{-\beta_N \ell}/2) + \cos(\beta_N \ell)]$$

For $\beta_N \ell = 17.2787595323$ (mode 6), $K_N = 1.000000063$. For a 16 bit word, the computer carries seven significant figures, and thus, would make $1 - K_6$ identically zero. $e^{\beta_N \ell}$ for mode 6 is on the order of 3×10^7 so that $(1 - K_6)e^{\beta_6 \ell}$ would have a significant contribution to sine and cosine functions. Double precision will not change with phenomena for higher modes, so a convergent solution must be sought. First, in the expression for K_N, let $\cos(\beta_N \ell) = -1/\cosh(\beta_N \ell)$ and use the identities relating cosh and sinh to obtain

$$K_N = [1 - (2e^{-\beta_N \ell}\sin(\beta_N \ell)/1 - e^{-2\beta_N \ell})][1 + e^{-2\beta_N \ell})/(1 - e^{-2\beta_N \ell})]$$

Substituting the series expansion

$$1/1 - U = 1 + U + U^2 + U^3 + \ldots$$

and letting

$$\gamma = 2(e^{-2\beta_N \ell} + e^{-4\beta_N \ell} + e^{-6\beta_N \ell} + \ldots$$

we have

$$K_N = (1 + \gamma) - (1 + \gamma)[2e^{-\beta_N \ell}\sin(\beta_N \ell)/1 - e^{-2\beta_N \ell}]$$

Now, defining

$$C_N = 1 - K_N = [2e^{-\beta_N \ell}\sin(\beta_N \ell)/1 - e^{-2\beta_N \ell}](1 + \gamma) - \gamma$$

and expanding $1/1 - e^{-2\beta_N \ell}$ in a series, we obtain

$$C_N = 2e^{-\beta_N \ell}\sin(\beta_N \ell)(1 + 3\gamma/2 + \gamma^2/2) - \gamma$$

This expression, along with that for γ, can be substituted into the mode shape expression, $\phi_N(x)$, to yield this equation

$$\phi_N(x) = e^{(\beta_N x - \beta_N \ell)}\sin(\beta_N \ell)(1 + 3\gamma/2 + \gamma^2/2) - (\gamma/2)e^{\beta_N x} +$$

$$(1 - C_N/2)e^{-\beta_N x} - \cos(\beta_N x) + (1 - C_N)\sin(\beta_N x)$$

This equation was programmed and values of $\phi_N(x)$ were compared to those tabulated in Reference 10. The comparison showed that this form provided a stable solution for $\phi_N(x)$ for the first 20 modes.

APPENDIX E - LISTING OF COMPUTER PROGRAM

```
    100•       OVERLAY(IMPACT,0,0)
    110•       PROGRAM IMPDA(INPUT,OUTPUT)
    120•       COMMON D,RP,U,BL,BU,T,R,NM,SPAN1,SPAN2,B(20),W(20),A(20),BU
MMV(90)
    130•      1,S,TIM,V(20),EPS(1000),TTIM
    140•C ***  THIS PROGRAM CALCULATES THE STRAIN IN A CANTILEVER BEAM
    150•C  UNDER IMPACT. IMPACT CAN BE TREATED AS I.C. OR FORCED VIBR.
    160•       BNM=ALL=AL=AM=AK=AA=NKK=1HN
    170•       B(1)=1.875104077**2.
    180•       B(2)=4.69409113**2.
    190•       B(3)=7.85475744**2.
    200•       B(4)=10.99554074**2.
    210•       B(5)=14.13716839**2.
    220•       B(6)=17.27875953**2.
    230•       B(7)=20.42035513**2.
    240•       B(8)=23.56194491**2.
    250•       B(9)=26.70353755**2.
    260•       B(10)=29.84513021**2.
    270•       B(11)=32.98672286**2.
    280•       B(12)=36.12831551**2.
    290•       B(13)=39.26990817**2.
    300•       B(14)=42.41150082**2.
    310•       B(15)=45.55309347**2.
    320•       B(16)=48.69468613**2.
    330•       B(17)=51.83627878**2.
    340•       B(18)=54.97787143**2.
    350•       B(19)=58.11946409**2.
    360•       B(20)=61.26105674**2.
    370•       JK=0
    380•       PRINT 152
    390•152    FORMAT(X,'MODEL OPTIONS ARE-',//,10X,'POINT I.C.-INITIAL VE
LOCITY
    400•      1AT A POINT     ',/10X,'AREA I.C.-INITIAL VELOCITY OVER AN AR
EA      '
    410•      1,/10X,'FORCED VIBRATION AT A POINT     ',/10X,'FORCED VIBRAT
ION OVE
    420•      1R AN AREA     ',/10X,'END')
    430•  178 PRINT 153
    440•153    FORMAT(X,'OPTION-')
    450•       READ 254,AB
    460•  254 FORMAT(A2)
    470•       IF(AB.EQ.1HE)GO TO 176
    480•154    FORMAT(A1)
    490•       PRINT*,'DO YOU WANT DAMPING?-'
    500•       READ 154,AD
    510•       IF(AA.EQ.1HY)GO TO 201
    520•  203 PRINT*,'HOW MANY MODES DO YOU WANT TO USE ? - '
    530•       READ*,NM
    540•       IF(BNM.EQ.1HY)GO TO 202
    550•  199 PRINT*,'ENTER THE DIMENSIONS, DENSITY, AND MODULUS OF YOUR
BEAM.'
    560•   25 PRINT*,'L,W,T,RHO,AND E - '
    570•       READ*,BL,BU,T,R,E
    580•       IF(AL.EQ.1HY)GO TO 202
    590•  205 PRINT*,'ENTER IMPACT POINT AND POINT FOR STRAIN CALCS IN %
OF L -
    600•      1'
..
```

```
      620.       SPAN1=SPAN1/100.
      630.       SPAN2=SPAN2/100.
      640.       IF(ALL.EQ.1HY)GO TO 202
      650.   200 PRINT*,'ENTER DIAMETER, DENSITY, AND VELOCITY OF THE PROJEC
     TILE -
      660.      1'
      670.       READ*,D,RP,V
      680.       IF(AK.EQ.1HY)GO TO 201
      690.206    PRINT*,'WHAT TIME PERIOD DO YOU WANT TO CALCULATE STRAIN OV
     ER?(500
      700.      1, 50, 5, OR 0.5 MS.) - '
      710.       READ*,TIM
      720.       TTIM=TIM
      730.       TIM=TIM*.001
      740.       IF(AKK.EQ.1HY)GO TO 19
      750.C  ***   CALCULATE RESONANT FREQUENCIES
      760.  202 C1=5.67157*T*SQRT(E/R)/BL**2.0
      770.       DO 6 I=1,NM
      780.       W(I)=B(I)*C1
      790.     6 CONTINUE
      800.  201 IF(AB.EQ.2HPI)CALL PIC
      810.       IF(AB.EQ.2HAI)CALL AIC
      820.       IF(AB.EQ.2HFV)CALL FV
      830.       IF(AB.EQ.2HFA)CALL FA
      840.C ********** CALCULATE STRAIN   **********
      850.       TO=D/(V*12.)
      860.    19 TI=0.
      870.       S=0.
      880.       IT=0.
      890.       DO 12 I=1,1000
      900.       TI=TI+.001*TIM
      910.       EPS(I)=0.
      920.       Z=0.
      930.       DO 13 J=1,NM
      940.       IF(J.EQ.1.AND.L.LE.9.)Z=0.001
      950.       IF(J.EQ.2.OR.J.EQ.3)Z=0.0005
      960.       IF(J.GE.4)Z=0.0015
      970.       IF(AD.EQ.1HN)Z=0.
      980.       IF(AB.EQ.2HFV)GO TO 75
      990.       IF(AB.EQ.2HFA)GO TO 75
     1000.       EPS1=Y(J)*SIN(W(J)*TI)*EXP(-Z*W(J)*TI)
     1010.       GO TO 13
     1020.    75 EPS1=Y(J)*(SIN(W(J)*TO)*SIN(W(J)*TI)-(1.-COS(W(J)*TO))*COS(
    W(J)*TI
     1030.      1))*EXP(-Z*W(J)*TI)
     1040.       IF(TI.LT.TO)EPS1=Y(J)*(1-COS(W(J)*TI))*EXP(-Z*W(J)*TI)
     1050.    13 EPS(I)=EPS(I)+EPS1
     1060.       EPS(I)=EPS(I)*T/2.
     1070.       IF(ABS(EPS(I)).GT.ABS(S))GO TO 41
     1080.       GO TO 12
     1090.    41 S=EPS(I)
     1100.       IT=I
     1110.    12 CONTINUE
     1120.C ********************  PRINT RESULTS  **********************
     1130.       TM=IT
     1140.       TM=TM*TIM*.001
     1150.       PRINT 300,S,TM
```

```
 1160*  200 FORMAT(2X,'THE MAX STRAIN IS ',E12.6,' OCCURRING AT ',E12.6
  SECO
 1170*      1NDS.')
 1180*       PRINT*,'      MODE    FREQUENCY, HZ.    COEFFICIENT    %:A,
IN.
 1190*      1VEL, F/S'
 1200*       DO 10 N=1,NM
 1210*       UD=W(N)/(2.*3.14159)
 1220*       A1=A(N)
 1230*       PRINT 101,N,UD,A1,D.V
 1240*  101 FORMAT(6X,I2.7X,E12.6,5X,E12.6,2X,E9.3,2X,E9.3)
 1250*   10 CONTINUE
 1260*   30 PRINT*,'PLOT? - '
 1270*      READ 154,AIJK
 1280*      IF(AIJK.EQ.1HY)GO TO 31
 1290*      GO TO 29
 1300*   31 CALL PLOT(EPS)
 1310*   29 PRINT*,'WOULD YOU LIKE THE SAME PROBLEM, DIFFERENT OPTION?
 '
 1320*      READ 154,AA
 1330*      IF(AA.EQ.1HY)GO TO 178
 1340*      PRINT*,'WOULD YOU LIKE TO CHANGE THE NUMBER OF MODES? - '
 1350*      READ 154,BNM
 1360*      IF(BNM.EQ.1HY)GO TO 203
 1370*      PRINT*,'WOULD YOU LIKE TO CHANGE THE TIME PERIOD? -'
 1380*      READ 154,AKK
 1390*      IF(AKK.EQ.1HY)GO TO 206
 1400*   27 PRINT*,'WOULD YOU LIKE THE SAME PROBLEM WITH DIFFERENT IMPA
CT OR S
 1410*      1TRAIN LOCATIONS? -'
 1420*       READ 154,ALL
 1430*       IF(ALL.EQ.1HY)GO TO 205
 1440*   22 PRINT*,'WOULD YOU LIKE THE SAME BEAM WITH A DIFFERENT PROJE
CTILE?
 1450*      1-'
 1460*       READ 154,AK
 1470*       IF(AK.EQ.1HY)GO TO 200
 1480*   23 PRINT*,'WOULD YOU LIKE A DIFFERENT BEAM WITH THE SAME PROJE
CTILE
 1490*      1? -'
 1500*       READ 154,AL
 1510*       IF(AL.EQ.1HY)GO TO 199
 1520*   24 PRINT*,'WOULD YOU LIKE A DIFFERENT BEAM AND DIFFERENT PROJE
CTILE
 1530*      1? -'
 1540*       READ 154,AM
 1550*       IF(AM.EQ.1HY)GO TO 199
 1560*       GO TO 178
 1570*176    CONTINUE
 1580*       END
 1590*       SUBROUTINE PLOT(X)
 1600*       COMMON D,RP,V,BL,BU,T,R,NM,SPAN1,SPAN2,B(20),W(20),A(20),DU
MMY(90)
 1610*      1,S,TIM,Y(20),EPS(1000),TTIM
 1620*       DIMENSION X(1000),IT(8)
 1630*       CALL INITT(120)
 1640*       IF(ABS(S).LT.0.0014215)YM=.5
```

```
1650.       IF(ABS(S).GT.0.0014215)YM=1.
1660.       IF(ABS(S).GT.0.002343)YM=2.
1670.       CALL WINDOW(0.,TIM,-YM,YM)
1680.       CALL SUBWDO(230,3200,280,2688)
1690.       TI=TIM*.001
1700.       CALL MOVEA(0.,0.)
1710.       DO 10 I=1,1000
1720.       X1=X(I)*2.-0.005686
1730.       CALL DRAWA(TI,X1)
1740.    10 TI=TI+TIM*.001
1750.       CALL MOVEA(0.,-YM)
1760.       CALL DRAWA(TIM,-YM)
1770.       CALL DRAWA(TIM,YM)
1780.       CALL DRAWA(0.,YM)
1790.       CALL DRAWA(0.,-YM)
1800.       CALL TSEND
1810.       R=TIM/5.
1820.       DO 11 I=1,4
1830.       CALL MOVEA(I*R,-YM)
1840.       CALL DRAWA(I*R,-YM+YM*.04)
1850.       CALL MOVEA(I*R,YM)
1860.    11 CALL DRAWA(I*R,YM-YM*.04)
1870.       CALL TSEND
1880.       R=-YM
1890.       DO 12 I=1,9
1900.       R=R+YM*.2
1910.       CALL MOVEA(0.,R)
1920.       CALL DRAWA(.02*TIM,R)
1930.       CALL MOVEA(TIM,R)
1940.    12 CALL DRAWA(TIM-.02*TIM,R)
1950.       CALL TSEND
1960.       J=262
1970.       CALL ANMODE
1980.       CALL CHRSIZ(4)
1990.       DO 13 I=1,6
2000.       CALL MOVABS(J,240)
2010.       IF(I.EQ.1)LBL=2H0.
2020.       IF(TTIM.EQ.500)GO TO 1001
2030.       IF(TTIM.EQ.50)GO TO 1002
2040.       IF(TTIM.EQ.5)GO TO 1003
2050.       IF(I.EQ.2)LBL=2H.1
2060.       IF(I.EQ.3)LBL=2H.2
2070.       IF(I.EQ.4)LBL=2H.3
2080.       IF(I.EQ.5)LBL=2H.4
2090.       IF(I.EQ.6)LBL=2H.5
2100.       GO TO 1100
2110. 1002  IF(I.EQ.2)LBL=2H10
2120.       IF(I.EQ.3)LBL=2H20
2130.       IF(I.EQ.4)LBL=2H30
2140.       IF(I.EQ.5)LBL=2H40
2150.       IF(I.EQ.6)LBL=2H50
2160.       GO TO 1100
2170. 1003  IF(I.EQ.2)LBL=2H1.
2180.       IF(I.EQ.3)LBL=2H2.
2190.       IF(I.EQ.4)LBL=2H3.
2200.       IF(I.EQ.5)LBL=2H4.
2210.       IF(I.EQ.6)LBL=2H5.
```

```
2220-       GO TO 1100
2230- 1001 IF(I.EQ.2)LBL=2H:0
2240-       IF(I.EQ.3)LBL=2H:0
2250-       IF(I.EQ.4)LBL=2H30
2260-       IF(I.EQ.5)LBL=2H40
2270-       IF(I.EQ.6)LBL=2H50
2280-       CALL AOUTST(2,LBL)
2290-       LBL=2H0.
2300-       IF(I.EQ.1)GO TO 1101
2310- 1100 CALL AOUTST(2,LBL)
2320- 1101 J=J+750
2330-    13 IF(I.EQ.5.AND.TTIM.EQ.500)J=J-60
2340-       J=280
2350-       DO 14 I=1,3
2360-       CALL MOVABS(220,J)
2370-       IF(S.GT.0.002843)GO TO 21
2380-       IF(S.LT.0.0014215)GO TO 22
2390-       IF(I.EQ.1)LBL=2H-1
2400-       IF(I.EQ.2)LBL=2H0.
2410-       IF(I.EQ.3)LBL=2H1.
2420-       GO TO 25
2430-    21 IF(I.EQ.1)LBL=2H-2
2440-       IF(I.EQ.2)LBL=2H0.
2450-       IF(I.EQ.3)LBL=2H2.
2460-       GO TO 25
2470-    22 IF(I.EQ.1)LBL=2H-5
2480-       IF(I.EQ.2)LBL=2H0.
2490-       IF(I.EQ.3)LBL=2H5.
2500-    25 CALL AOUTST(2,LBL)
2510-       CALL CHRSIZ(3)
2520-    14 J=J+1344
2530-       CALL TSEND
2540-       CALL MOVABS(2000,140)
2550-       DO 50 I=1,4
2560-       IT(1)=2HTI
2570-       IT(2)=2HME
2580-       IT(3)=2H,M
2590-       IT(4)=2HS.
2600-50    CALL AOUTST(2,IT(I))
2610-       CALL MOVABS(80,3088)
2620-       DO 51 I=1,5
2630-       IT(1)=2HST
2640-       IT(2)=2HRA
2650-       IT(3)=2HIN
2660-       IT(4)=2H,V
2670-       IT(5)=1H.
2680-       IF(S.LT.0.0014215)IT(5)=2H-1
2690-       IF(S.LT.0.0014215)N=10
2700-51    CALL AOUTST(2,IT(I))
2710-       CALL HOME
2720-       CALL HDCOPY
2730-       CALL CHRSIZ(2)
2740-       CALL ERASE
2750-       CALL FINITT
2760-       RETURN
2770-       END
2780-       SUBROUTINE FV
```

```
 2790•      COMMON D,RP,V,BL,BU,T,R,NM,SPAN1,SPAN2,B(20),W(20),A(20),DU
MMY(50)
 2800•     1,S,TIM,Y(20)
 2810•      DIMENSION C(20)
 2820•C  ***** CALCULATE CONSTANTS
 2830•  201 PM=3.14159*D**3.*RP/6.
 2840•      TO=D/(V*12.)
 2850•      BI=BU*T**3./12.
 2860•C  ********** CALCULATE Y(N)'S ****************** **********
**
 2870•      DO 9 N=1,NM
 2880•      B1=SQRT(B(N))
 2890•      G=2.*(EXP(-2.*B1)+EXP(-4.*B1)+EXP(-6.*B1)+EXP(-8.*B1))
 2900•      C(N)=-G+(2.*SIN(B1)*EXP(-B1)*(1.+G))/(1.-EXP(-2.*B1))
 2910•      ARG=B1*SPAN1
 2920•      Y(N)=EXP(ARG-B1)*SIN(B1)*(1.+3.*G/2.+G**2./2.)-G*EXP(ARG)/2
.*(1.-C
 2930•     1(N)/2.)*EXP(-ARG)-COS(ARG)+(1.-C(N))*SIN(ARG)
 2940•    9 CONTINUE
 2950•C  ********** CALCULATE CS ***************
 2960•      CS=0.
 2970•      DO 17 I=1,NM
 2980•      TEMP=Y(I)*(1.-C(N))*SIN(W(I)*TO)/(W(I)*SQRT(B(I)))
 2990•  151 FORMAT(E12.6)
 3000•   17 CS=CS+TEMP
 3010•C  ********** CALCULATE A'S ************************
 3020•      DO 3 I=1,NM
 3030•      A(I)=6.*PM*V*Y(I)/(CS*R*BU*BL*T*W(I)**2.)
 3040•    8 CONTINUE
 3050•C  ********** CALCULATE COEFFICIENTS FOR STRAIN **********
****
 3060•      DO 11 N=1,NM
 3070•      B2=SQRT(B(N))
 3080•      B1=SQRT(B(N))*SPAN2
 3090•      G=2.*(EXP(-2.*B2)+EXP(-4.*B2)+EXP(-6.*B2)+EXP(-8.*B2))
 3100•      SUM=EXP(B1-B2)*SIN(B2)*(1.+3.*G/2.+G**2./2.)-G*EXP(B1)/2.+(
1.-C(N)
 3110•     1/2.)*EXP(-B1)+COS(B1)-(1.-C(N))*SIN(B1)
 3120•   11 Y(N)=SUM*A(N)*B(N)/BL**2.
 3130•      RETURN
 3140•      END
 3150•      SUBROUTINE PIC
 3160•      COMMON D,RP,V,BL,BU,T,R,NM,SPAN1,SPAN2,B(20),W(20),A(20),DU
MMY(30)
 3170•     1,S,TIM,Y(20)
 3180•      DIMENSION C(20)
 3190•C  ***** CALCULATE CONSTANTS
 3200•  231 PM=3.14159*D**3.0*RP/6.0
 3210•      BM=BL*BU*T*R
 3220•      C2=PM*V*12.0/BM
 3230•C  ********** CALCULATE Y(N)'S ****************** **********
**
 3240•      DO 9 N=1,NM
 3250•      B1=SQRT(B(N))
 3260•      G=2.*(EXP(-2.*B1)+EXP(-4.*B1)+EXP(-6.*B1)+EXP(-8.*B1))
 3270•      C(N)=-G+(2.*SIN(B1)*EXP(-B1)*(1.+G))/(1.-EXP(-2.*B1))
 3280•      ARG=B1*SPAN1
```

```
      Y(N)=EXP(ARG-B1)*SIN(B1)*(1.+3.*G/2.+G**2./8.)-G*EXP(-ARG)*(
     +1.-C
     1(N)/2.)*EXP(-ARG)-COS(ARG)+(1.-C(N))*SIN(ARG)
    9 CONTINUE
C   ********************  CALCULATE CS  ****************************
      CS=0.
      DO 4 I=1,NM
      TEMP=Y(I)*2.*(1.-C(N))/SQRT(B(I))
    4 CS=CS+TEMP
C   ********************  CALCULATE A'S  ***************************
      DO 8 I=1,NM
      A(I)=C2*Y(I)/(CS*U(I))
    8 CONTINUE
C   ********************  CALCULATE COEFFICIENTS FOR STRAIN *********
****
      DO 11 N=1,NM
      B2=SQRT(B(N))
      B1=SQRT(B(N))*SPAN2
      G=2.*(EXP(-2.*B2)+EXP(-4.*B2)+EXP(-6.*B2)+EXP(-8.*B2))
      SUM=EXP(B1-B2)*SIN(B2)*(1.+3.*G/2.+G**2./2.)-G*EXP(B1)/2.+(
     1.-C(N)
     1/2.)*EXP(-B1)+COS(B1)-(1.-C(N))*SIN(B1)
   11 Y(N)=SUM*A(N)*B(N)/BL**2.
      RETURN
      END
      SUBROUTINE AIC
      COMMON D,PP,U,BL,BU,T,R,NM,SPAN1,SPAN2,B(20),U(20),A(20),DU
     1MY(90)
     1,S,TIM,Y(20)
      DIMENSION C(20)
C     *****   CALCULATE CONSTANTS
  201 PM=3.14159*D**3.0*RP/6.0
      BM=BL*BU*T*R
      C2=PM*U*12.0/BM
C     ***********  CALCULATE Y(N)'S  ********************  ***********
**
      DO 9 N=1,NM
      B1=SQRT(B(N))
      G=2.*(EXP(-2.*B1)+EXP(-4.*B1)+EXP(-6.*B1)+EXP(-8.*B1))
      C(N)=-G+(2.*SIN(B1)*EXP(-B1)*(1.+G))/(1.-EXP(-2.*B1))
      A1=B1*(SPAN1+0.5*D/BL)
      A2=B1*(SPAN1-0.5*D/BL)
      Y(N)=(0.5*C(N)*(EXP(A1)-EXP(A2))-(1.-0.5*C(N))*(EXP(-A1)-EX
     P(-A2))
     1-SIN(A1)+SIN(A2)-(1.-C(N))*(COS(A1)-COS(A2)))*BL/B1
    9 CONTINUE
C   ********************  CALCULATE CS  ****************************
      CS=0.
      DO 4 I=1,NM
      TEMP=Y(I)*2.*(1.-C(N))/SQRT(B(I))
    4 CS=CS+TEMP
C   ********************  CALCULATE A'S  ***************************
      DO 8 I=1,NM
      A(I)=C2*Y(I)/(CS*U(I))
    8 CONTINUE
C   ********************  CALCULATE COEFFICIENTS FOR STRAIN *********
****
```

```
      DO 11 N=1,NM
      B2=SQRT(B(N))
      B1=SQRT(B(N))*SPAN2
      G=2.*(EXP(-2.*B2)+EXP(-4.*B2)+EXP(-6.*B2)+EXP(-8.*B2))
      SUM=EXP(B1-B2)*SIN(B2)*(1.+3.*G/2.+G**2./2.)-G*EXP(B1)/8.*(
1.-C(N)
     1/2.)*EXP(-B1)+COS(B1)-(1.-C(N))-SIN(B1)
   11 Y(N)=SUM*A(N)*D(N)/BL**2.
      RETURN
      END
      SUBROUTINE FA
      COMMON D,RP,V,BL,BW,T,R,NM,SPAN1,SPAN2,B(20),U(20),A(20),DU
MMY(60)
     1,S,TIM,Y(20)
      DIMENSION C(20)
C*****    CALCULATE CONSTANTS    **************
  201 PM=3.14159*D**3.*RP/6.
      TO=D/(V*12.)
      BI=BW*T**3./12.
C**********   CALCULATE Y(N)'S  **********
      DO 9 N=1,NM
      B1=SQRT(B(N))
      G=2.*(EXP(-2.*B1)+EXP(-4.*B1)+EXP(-6.*B1)+EXP(-8.*B1))
      C(N)=-G+(2.*SIN(B1)*EXP(-B1)*(1.+G))/(1.-EXP(-2.*B1))
      A1=B1*(SPAN1+0.5*D/BL)
      A2=B1*(SPAN1-0.5*D/BL)
      Y(N)=(0.5*C(N)*(EXP(A1)-EXP(A2))-(1.-0.5*C(N))*(EXP(-A1)-EX
P(-A2))
     1-SIN(A1)+SIN(A2)-(1.-C(N))*(COS(A1)-COS(A2)))*BL/B1
    9 CONTINUE
C**************   CALCULATE CS   ****************
      CS=0.
      DO 17 I=1,NM
      TEMP=Y(I)*(1.-C(N))*SIN(U(I)*TO)/(U(I)*SQRT(B(I)))
   17 CS=CS+TEMP
C*********  CALCULATE  A'S   **********
      DO 8 I=1,NM
      A(I)=6.*PM*V*Y(I)/(CS*R*BW*BL*T*W(I)**2.)
    8 CONTINUE
C************ CALCULATE COEFFICIENTS FOR STRAIN  *****
      DO 11 N=1,NM
      B2=SQRT(B(N))
      B1=SQRT(B(N))*SPAN2
      G=2.*(EXP(-2.*B2)+EXP(-4.*B2)+EXP(-6.*B2)+EXP(-8.*B2))
      SUM=EXP(B1-B2)*SIN(B2)*(1.+3.*G/2.+G**2./2.)-G*EXP(B1)/2.+(
1.-C(N)
     1/2.)*EXP(-B1)+COS(B1)-(1.-C(N))*SIN(B1)
   11 Y(N)=SUM*A(N)*B(N)/BL**2.
      RETURN
      END
**
```

```
      SUBROUTINE FU
      COMMON D,PP,V,BL,SU,T,B,NM,SPAN1,SPAN2,B(20),U(20),A(20),SU
NRV(20)
     1,S,TIM,Y(20),EPS(1000),TTIM,E
      DIMENSION C(20)
C*****   CALCULATE CONSTANTS
  201 PM=3.14159*D**3.*PP/6.
      TO=D/(V*12.)
      BI=SU*T**3./12.
C**********  CALCULATE Y(N)'S  ********************  **********
**
      DO 9 N=1,NM
      B1=SQRT(B(N))
      G=2.*(EXP(-2.*B1)+EXP(-4.*B1)+EXP(-6.*B1)+EXP(-8.*B1))
      C(N)=-G+(2.*SIN(B1)*EXP(-B1)*(1.+G))/(1.-EXP(-2.*B1))
      ARG=B1*SPAN1
      Y(N)=EXP(ARG-B1)*SIN(B1)*(1.+3.*G/2.+G**2./2.)-G*EXP(ARG)/2
.*(1.-C
     1(N)/2.)*EXP(-ARG)-COS(ARG)+(1.-C(N))*SIN(ARG)
    9 CONTINUE
C**********   CALCULATE CS   **************
      CS=0.
      DO 17 I=1,NM
      BS=SQRT(B(I))/BL
      TEMP=(1.+COS(U(I)*TO))*(1.-C(I))*Y(I)/(BS*(U(I)**2.+3.14159
**2./TO
     1**2.))
   17 CS=CS+TEMP
C***************  CALCULATE A'S  ***********************
      DO 8 I=1,NM
      A(I)=PM*D*Y(I)/(2*3.14159*R*SU*T*CS*(U(I)**2.+3.14159**2./T
O**2.))
    8 CONTINUE
C***************  CALCULATE COEFFICIENTS FOR STRAIN *********
***
      DO 11 N=1,NM
      B2=SQRT(B(N))
      B1=SQRT(B(N))*SPAN2
      G=2.*(EXP(-2.*B2)+EXP(-4.*B2)+EXP(-6.*B2)+EXP(-8.*B2))
      SUM=EXP(B1-B2)*SIN(B2)*(1.+3.*G/2.+G**2./2.)-G*EXP(B1)/2.+(
1.-C(N)
     1/2.)*EXP(-B1)+COS(B1)-(1.-C(N))*SIN(B1)
   11 Y(N)=SUM*A(N)*B(N)/BL**2.
      RETURN
      END
```

```
 3910.      SUBROUTINE FA
 3920.      COMMON B,EP,V,BL,BU,T,R,NM,SPAN1,SPAN2,B(80),W(80),A(80),DU
MMY(90)
 3930.     1,S,TIR,Y(20)
 3940.      DIMENSION C(20)
 3950.C   ***** CALCULATE CONSTANTS ***************
 3960.  201 PM=3.14159*D**3.*EP/6.
 3970.      TO=D/(V*12.)
 3980.      BI=BU*T**3./12.
 3990.C  ************ CALCULATE Y(N)'S ************
 4000.      DO 9 N=1,NM
 4010.      B1=SQRT(B(N))
 4020.      G=2.*(EXP(-2.*B1)+EXP(-4.*B1)+EXP(-6.*B1)+EXP(-8.*B1))
 4030.      C(N)=-G+(2.*SIN(B1)*EXP(-B1)*(1.+G))/(1.-EXP(-2.*B1))
 4040.      A1=B1*(SPAN1+0.5*D/BL)
 4050.      A2=B1*(SPAN1-0.5*D/BL)
 4060.      Y(N)=(0.5*C(N)*(EXP(A1)-EXP(A2))-(1.-0.5*C(N))*(EXP(-A1)-EX
P(-A2))
 4070.     1-SIN(A1)+SIN(A2)-(1.-C(N))*(COS(A1)-COS(A2)))*BL/B1
 4080.    9 CONTINUE
 4090.C   ************ CALCULATE CS ************
 4100.      CS=0.
 4110.      DO 17 I=1,NM
 4120.      BS=SQRT(B(I))/BL
 4130.      TEMP=(1.+COS(W(I)*TO))*(1.-C(I))*Y(I)/(BS*(W(I)**2.+3.14159
**2./TO
 4140.     1**2.))
 4150.   17 CS=CS+TEMP
 4160.C   ********** CALCULATE A'S **********
 4170.      DO 8 I=1,NM
 4180.      A(I)=PM*D*Y(I)/(2*3.14159*CS*B*BU*T*(W(I)**2.+3.14159**2./T
O**2.))
 4190.    8 CONTINUE
 4200.C  ********** CALCULATE COEFFICIENTS FOR STRAIN *****
 4210.      DO 11 N=1,NM
 4220.      B2=SQRT(B(N))
 4230.      B1=SQRT(B(N))*SPAN2
 4240.      G=2.*(EXP(-2.*B2)+EXP(-4.*B2)+EXP(-6.*B2)+EXP(-8.*B2))
 4250.      SUM=EXP(B1-B2)*SIN(B2)*(1.+3.*G/2.+G**2./2.)-G*EXP(B1)/2.+(
1.-C(N)
 4260.     1/2.)*EXP(-B1)+COS(B1)-(1.-C(N))*SIN(B1)
 4270.   11 Y(N)=SUM*A(N)*B(N)/BL**2.
 4280.      RETURN
 4290.      END
..
```

REFERENCES

1. "Deflections and Stresses in Simply Supported Beams Under Impact Loading," M. Paloas, J. Inst. Eng. Civ. Eng. Div., Vol 57, July 1974.

2. "Experiment on the Impact Loading of a Cantilever (Deflection Measurement)," H. B. Sutton, Int. J. Mech. Eng. Educ., Vol 2, No. 3, July 1974.

3. "Experimental Techniques for Analysis of Transverse Impact on Beams," Thomas H. Berns, Naval Postgraduate School, June 1969.

4. "Mechanical Design Analysis," M. F. Spotts, Prentice-Hall, 1964.

5. "Theory of Vibration with Applications," Wm. T. Thompson, Prentice-Hall, 1972.

6. "Behavior of Cantilever Beam Under Impact by a Soft Projectile," S. W. Tsai, C. T. Sun, A. K. Hopkins, H. T. Hahn, and T. W. Lee, AFML-TR-74-94, November 1974.

7. "Impact Behavior of Low Strength Projectiles," James S. Wilbeck, AFML-TR-77-134, July 1978.

8. "Test Methodology Correlation for Foreign Object Damage," T. Wong and Robert W. Cornell, AFML-TR-78-16, March 1978.

9. "Impact: The Theory and Physical Behavior of Colliding Solids," W. Goldsmith, Edward Arnold Publishers, 1960.

10. "The Mechanics of Vibration," R. E. D. Bishop and D. C. Johnson, Cambridge U. Press, 1960.

*U.S.Government Printing Office: 1980 — 657-084/731


DAT
FILM
8-8